National Library of Canada

Acquisitions and Bibliographic Services Branch

395 Wellington Street
Ottawa, Ontario
K1A 0N4

Bibliothèque nationale du Canada

Direction des acquisitions et des services bibliographiques

395, rue Wellington
Ottawa (Ontario)
K1A 0N4

Your file Votre référence

Our file Notre référence

NOTICE

The quality of this microform is heavily dependent upon the quality of the original thesis submitted for microfilming. Every effort has been made to ensure the highest quality of reproduction possible.

If pages are missing, contact the university which granted the degree.

Some pages may have indistinct print especially if the original pages were typed with a poor typewriter ribbon or if the university sent us an inferior photocopy.

AVIS

La qualité de cette microforme dépend grandement de la qualité de la thèse soumise au microfilmage. Nous avons tout fait pour assurer une qualité supérieure de reproduction.

S'il manque des pages, veuillez communiquer avec l'université qui a conféré le grade.

La qualité d'impression de certaines pages peut laisser à désirer, surtout si les pages originales ont été dactylographiées à l'aide d'un ruban usé ou si l'université nous a fait parvenir une photocopie de qualité inférieure.

Canada

Procedures for basic inverse problems

Black body radiation problem and phonon density of states problem

by

Lixin Dou

Thesis submitted to the Graduate studies of
the University of Ottawa
in
partial fulfilment of the requirements
for the degree of Master of Science
in
Physics

Department of Physics
Faculty of Science
University of Ottawa

ISBN 0-315-85757-9

Canada

UNIVERSITÉ D'OTTAWA
UNIVERSITY OF OTTAWA

Acknowledgements

I would like to take this opportunity to express my sincere gratitudes to my thesis supervisor Dr. R. J. W. Hodgson for his encouragement, advice, help and kindness throughout the course of this work. I must say that it was Dr. Hodgson who gave me the opportunity to get into University of Ottawa and pursue my research.

I would like to thank Dr. Benson, R. Chagnon, B. Chen and H. Lacasse for their help with my teaching works. I would also thank the following friends in the Department of Physics who helped make life, study and work more bearable and joyful during my Master's research: Renfang Tu, Yang Cai, Qiang Ren, Ye Wang, Jinglei Meng, Sean Wang, Robert Parent, Pamela Tume and David Leblanc, as well as the professors, the secretaries and staff of the department.

Dedicated to my Mother, my Father, and
my dear Husband Ping,
who made all this possible.

Abstract

Two numerical procedures, the regularization method and the maximum entropy method, have been investigated and developed to solve some basic inverse problems in theoretical physics. Both of them are applied to the inverse black body radiation problem and the inverse phonon density of states problem. The inverse black body radiation problem is concerned with the determination of the area temperature distribution of a black body source from spectral measurements of its radiation. The phonon density of states problem is defined to be the determination of the phonon density of states function from the measured lattice specific heat function at constant volume. Those problems are ill-posed and can be expressed as a Fredholm integral equation of the first kind. It appears that both the regularization method and the maximum entropy method are successful in solving the two ill-posed problems. Generally the two procedures can be applied to any inverse problem which belongs to the class of the Fredholm integral equation of the first kind.

Table of Contents

CHAPTER ONE

Introduction

Many important practical problems in theoretical physics, such as the inverse black body radiation problem and the phonon density of states problem, lead to ill-posed problems in mathematics. Because of some inherent ill conditioning in these problems, solving them theoretically and numerically is very difficult. During the last three to four decades, a lot of attention has been paid to these problems and some remarkable methods have been developed. This thesis will present the results obtained during the past year and a half while working on the investigation and comparison of the regularization and maximum entropy techniques to solve the inverse black body radiation problem and the phonon density of states problem in physics. Two journal papers have been written as a result of this work.

The regularization method, which resulted in the replacement of the ill-posed problem by a well-posed problem, was first proposed theoretically by Tikhonov[1-2] to solve ill-posed problem in 1960's. Phillips[3] presented the application of this method to

the Fredholm integral equation of the first kind. Recently, this method was introduced to solve the black body radiation problem by Sun and Jaggard[4] and some encouraging results were obtained. But their work is only a simple application of the regularization technique. Further investigation about this method is still quite necessary. Details will be given in Chapter Three. Maximum entropy was first introduced by Shannon[5] in the 1940's as a concept to describe the information content in a signal. Since then it has been successfully applied to a number of areas such as digital signal and image processing, and geophysical data analysis. It is the first time that the maximum entropy method as an alternative procedure is applied to solve the inverse black body radiation problem and the phonon density of states problem. We will give details about this method in Chapter Five.

In this chapter, the statements about the inverse black body radiation problem and the inverse phonon density of states problem will be given. Both of these problems can be treated as Fredholm integral equations of the first kind. The basic ideas about Fredholm integral equations of the first kind will be introduced. An extensive review of previous work on these two problems will be presented in Chapter Two. In Chapter Three a procedure called the regularization method will be introduced in detail and some very good results for the black body radiation problem and the phonon density of states problem will be demonstrated. The maximum entropy method and its applications to the black body problem and the phonon density problem will be presented in Chapter Four. For comparisons with the regularization and maximum entropy, an alternative Laplace transform method and its application to the black body radiation problem will be shown in Chapter Five. In Chapter Six, the nature of the results achieved by these different methods will be discussed, and conclusions presented.

1. Black body radiation problem

The power spectrum P(ν,T) radiated per unit area of a black body with absolute temperature T is given by Planck's law as

$$P(\nu,T) = \frac{2\,h\nu^3}{c^2}\,\frac{1}{e^{h\nu/kT} - 1} \qquad (1.1)$$

where

h = Planck's constant

k_B = Boltzmann's constant

c = Velocity of light

If the area-temperature distribution of the black body is a(T), then the total radiated power spectrum W(ν) is

$$W(\nu) = \frac{2\,h\nu^3}{c^2}\int_0^{\infty}\frac{a(T)\,dT}{e^{h\nu/kT} - 1} \qquad (1.2)$$

The inverse black body radiation problem is defined to be the determination of the temperature distribution a(T) given the measured radiated power spectrum W(ν). This consists of solving the integral equation (1.1) for the area-temperature distribution a(T). In practice, when T => 0 or T => ∞, a(T) => 0, so that the range of the integration can be restricted:

$$W(\nu) = \frac{2\,h\nu^3}{c^2} \int_{T_1}^{T_2} \frac{a(T)\,dT}{e^{h\nu/kT} - 1} \tag{1.3}$$

By defining

$$G(\nu) = \frac{c^2}{2\,h\nu^3} W(\nu), \tag{1.4}$$

then

$$G(\nu) = \int_{T_1}^{T_2} \frac{a(T)\,dT}{e^{h\nu/kT} - 1} \tag{1.5}$$

This form is that of a Fredholm integral equation of the first kind:

$$\int_a^b k(x,y)\, f(y)\, dy = g(x) \qquad c \le x \le d$$

So, the inverse black body radiation problem can be dealt with as a Fredholm integral equation of the first kind.

2. Phonon density of states problem

The temperature dependence of the harmonic phonon specific heat $C_v(T)$ is uniquely determined by the phonon density of states function $g(\omega)$ through the relation:

$$C_v(T) = r\,k \int_0^\infty \frac{(\hbar\omega/kT)^2\, e^{\hbar\omega/kT}}{(e^{\hbar\omega/kT} - 1)^2} g(\omega) d\omega \qquad (1.6)$$

where

$\hbar$ = Planck's constant

k_B = Boltzmann's constant

Eq.(1.6) holds for a crystalline lattice with r atoms per unit cell.

The inverse phonon density of states problem is defined to be the determination of the phonon density of states function $g(\omega)$ from the measured lattice specific heat function at constant volume $C_v(T)$. Then the specific heat for one mole will be:

$$C_v(T) = N_0\, k \int_0^{\infty} \frac{(\hbar\omega/kT)^2\, e^{\hbar\omega/kT}}{(e^{\hbar\omega/kT} - 1)^2} g(\omega)d\omega \qquad (1.7)$$

For most crystalline lattices, the circular frequency goes from $0 - 5\times10^{13}$ rad./s. By defining:

$$G_v(T) = \frac{C_v(T)}{N_0\, k}, \qquad (1.8)$$

then

$$G_v(T) = \int_0^{\omega_m} \frac{(\hbar\omega/kT)^2 e^{\hbar\omega/kT}}{(e^{\hbar\omega/kT} - 1)^2} g(\omega)d\omega \qquad (1.9)$$

This is just the Fredholm integral equation of the first kind.

3. Fredholm integral equation of the first kind

By a Fredholm integral equation of the first kind is meant an equation of the form

$$\int_a^b k(x,y)\, f(y)\, dy = g(x) \qquad c \le x \le d \qquad (1.10)$$

Where g(x) is a given function (usually called the data), k(x,y) is a given function (the kernel of the equation) and f(y) is the unknown function.

Several observations concerning this equation come immediately to mind. The first is that the function g inherits some of the smoothness of the kernel k and therefore a solution may not exist if g is too roughly behaved. For example, if the kernel k is continuous and f is integrable, then it is easy to see that the function g defined by (1.10) is also continuous and hence if the given function g is not continuous, while the kernel is, then (1.10) can have no integrable solution. This is simply to say that the condition of existence of a solution is not trivial.

Another point to consider is the uniqueness of solutions. For example, if k(x,y) = x sin(y), then the function f(y)=1/2 is a solution of

$$\int_0^{\pi} k(x,y)\, f(y)\, dy = x \qquad (1.11)$$

but so are each of the functions $f_n(y)=1/2+\sin(ny)$, n=1, 2, 3,....

A more serious concern arises from the Riemann-Lebesgue lemma which states that if k(x,y) is any square integrable kernel, then

$$\int_0^{\pi} k(x,y)\sin(ny)dy \quad => 0 \quad \text{as} \quad n => \infty$$

From this it follows that if f is a solution of (1.10) and A is arbitrarily large, then

$$\int_0^{\pi} k(x,y)\,(f(y)+A\sin(ny))\,dy \quad => g(x) \qquad \text{as} \quad n => \infty$$

Therefore for large values of n the slightly perturbed data

$$\tilde{g}(x)=g(x)+A\int_0^{\pi} k(x,y)\sin(ny)\,dy$$

corresponds to a solution f(y)+Asin(ny) which differs markedly from f(y). So, in the Fredholm integral equation of the first kind, solutions generally depend discontinuously upon the data.

At the beginning of this century Hadamard[6] formalized the concept of well-posedness for such equations as follows: equation (1.10) is said to be well-posed if:

(a) For each $g \in G$, there exists a solution $f \in F$;

(b) The solution of (1.10) is unique;

(c) The solution of (1.10) depends continuously on the data g.

An equation of the type (1.10) which is not well-posed is called ill-posed. So,

generally Fredholm integral equations of the first kind are ill-posed problem.

Here, the inverse black body radiation problem and the phonon density of states problem are concrete physics problems. Obviously the first and second conditions above are satisfied in these two problems. So, the main goal of this work is to develop numerical procedures to solve these problems with stable solutions.

CHAPTER TWO

Review of Previous Work

1. Previous work on inverse black body radiation problem

The first formulation of the inverse black body radiation problem was proposed by Bojarski[7] in 1982. A numerical solution was presented using the inverse Laplace transform and an iterative process. In his work, a normalized absolute "coldness" was introduced to replace the temperature and the denominator of the integrand was expanded in a series, the integral equation was then converted to a form which could be treated as a Laplace transform. By implementing the inverse Laplace transform of the power spectrum, a function which depends only on the unknown area-coldness distribution could be found. Using an iterative process, the sought area-coldness distribution was reconstructed from this function (Equations of Bojarski's method will be introduced in Chapter Five). Following Bojarski's work, various authors[7-15] provided different improvements in both theoretical and numerical aspects based on his solution. Hamid and

Ragheb[8](1983) employed the Ragleigh-Jeans approximation to yield the corresponding area-coldness distribution using the inverse Laplace transform, but avoiding the iterative procedure because of the approximation. Only the low coldness part was reconstructed. Bojarski[9](1984) showed that Hamid-Ragheb failed to point out and/or recognize that their solution was not an inverse Rayleigh-Jeans approximation solution, but a far superior approximation. It turned out to be an acceptable approximation even for high frequencies. He also calculated the errors for different approximations with respect to the Planck's radiation law and introduced a closed form approximation to inverse black body radiation problem which was valid in Wien's regime. Later M. Lakhtakia and A. Lakhtakia[10] (1984) gave their closed form solution for the inverse Wien regime. Comments by Bojarski, Lakhtakia et al.[11](1985) clarified the point that the inverse Wien's regime is the first term in Bojarski's iterative procedure. Bojarski claimed that the iterative procedure is very simple and converges in about three iterations. Hunter[12](1986) derived an approximate formula for Planck's law which is more accurate at microwave frequencies than in the Rayleigh-Jeans and Hamid-Ragheb approximations. His formula led to an improved closed form approximation to the inverse black body problem in the microwave region. In 1987, Ragheb and Hamid [13] modified their first formula to obtain a new approximation for the Planck's radiation law valid at all frequencies. They claimed their modified approximation to Planck's law is more suitable than all other approximations at all frequencies.

An exact closed-form reconstruction algorithm has been given in terms of an infinite series by Kim and Jaggard.[14] in 1985. Instead of the iteration in Bojarski's[7] work, the area-coldness distribution can be reconstructed from an infinite series of a function which is the inverse Laplace transform of the power spectrum. Recently, Chen[15] proposed a new theorem for the inverse formula based on number theory. His

work is very similar to Kim's. The only difference is that Chen introduced the Moebius function $\mu(n)$ and expressed the area-coldness distribution as an infinite series composed of the function which is the inverse Laplace transform of the power spectrum. The coefficients in the series involve the Moebius function. Actually, Kim's infinite series is the same as Chen's, but he didn't realize that the coefficients are somehow connected with the Moebius function. So we can say that Chen's work is more theoretical than Kim's. All these methods described above involved the use of the inverse Laplace transform, even the modified Moebius inverse formula of Chen. In all of the works mentioned above only few very simple numerical examples were presented. Actually each of these solutions suffers from a defect with regard to their numerical implementation. As we described in Chapter One, the inverse black body radiation problem is an inherently ill-posed problem. Converting the original problem into an inverse Laplace transform problem can not help us to get rid of the ill-conditioned nature of the problem, because inverting a Laplace transform is also an ill-posed problem. Therefore, finding the inverse Laplace transform which is converted from the original problem is not numerically easier than solving the original equation. If we could have found a numerical method which can solve the inverse Laplace transform very well, using either the iterative process or the modified Moebius inverse formula, we could reconstruct the area-coldness distribution very precisely. We will see this in Chapter Five.

As far as the ill-conditioning is concerned, a numerical approach to obtain stable solutions for the inverse black body radiation problem was given by Sun and Jaggard[4] based on the Tikhonov regularization method. As can be seen in Fig. 2.1 this is a good alternative for dealing with this problem. Actually the Tikhonov regularization method is just designed to deal with those ill conditions involved in ill-posed problems. However their work is not very complete. They didn't pay any attention to how the regularization

operator affects the result. It is still necessary that more research be done with this method. Recently, Chen and Li[16] proposed a new method for solving the problem. This method is very similar to the method which was introduced by Montroll[17] to solve the inverse phonon density of states problem in 1942. In his work, the original integral equation was modified to a new version by introducing two new variables as

$$e^x = h\nu/kT_0, \qquad e^y = T/T_0,$$

where T_0 is an appropriate reference temperature. Then the original integral equation (1.5) can be rewritten as

$$G(x) = \int_{-\infty}^{\infty} \Phi(x - y)\, A(y)\, dy = \Phi(y) * A(y) \qquad (2.1)$$ with

$$G(x) = \frac{h^2c^2}{2k^3T_0^4}\, W\left(\frac{kT_0e^x}{h}\right)e^{-(2-\Delta)x}$$

$$A(y) = e^{(2+\Delta)y}\, a(T_0e^y), \qquad \Phi(u) = \frac{e^{(1+\Delta)u}}{e^{e^u} - 1}$$

which can be solved based on Fourier deconvolution. Some quite good results were obtained in Fig. 2.2 by Chen. However, it should be realized that there are some practical shortcomings in the process of deconvolution. The process is generally quite sensitive to noise in the input data. Sometimes quite reasonable attempts at deconvolution can produce nonsense for these reasons.

2. Previous work on inverse phonon density of states problem

There have been extensive studies related to the extraction of information about the phonon density of states from specific heat measurements since the 1940's. Montroll[17] theoretically solved the problem by the method of Fourier transforms which involves complex functions in 1942. Two substitutions were made in his formulations, then the equation (1.9) can be converted to a form which can be solved by Fourier deconvolution, which we will show later in this section. As both advanced computer techniques and the Fast Fourier Transform(FFT) were not available until 1960, this solution was not used for any numerical calculation. Grayson-Smith and Stanley[18] (1950) have shown that the phonon density of states $g(\omega)$ can be expressed as a Fourier series with coefficients derived from the specific heat. But this method is appropriate only when low-temperature data of the specific heat are used. Following Stanley's work, Kroll[19](1952) proposed a method which allows one to express the phonon density of states function $g(\omega)$ by a real function. But there was no numerical examples given in his work. Weiss[20](1959) developed another method in which the frequency spectrum was arbitrarily approximated by a polynomial and showed that the coefficient of the term T^{2n} in a low-temperature expansion of $C_v(T)/T$ in power of T^2 is related to the coefficient of the term ω^{2n} in the expansion of $g(\omega)$ in powers of ω^2. He admitted this method was not

very useful because the limits of experimental precision was not narrow enough. In practice, his method only provides useful information on the low-frequency end of the spectrum. Chambers[21](1961) considered the inversion of an expression equivalent to (1.7) but with the specific heat terms replaced by their higher order temperature derivatives, which converge more rapidly at high temperature. He showed that there is little benefit in going beyond the first derivative, and using a trial and error method demonstrates that a spectrum can be obtained but with poor resolution. None of the procedures mentioned above has been applied successfully to the determination of the phonon density of states for a real system. A procedure which is simpler but which has a comparable resolution to the above methods is to approximate $g(\omega)$ by a histogram comprising typically three Debye and/or Einstein distributions, the amplitude of each term being determined by a least-squares fit to $C_v(T)$ (Junod, Jarlborg et al.[22], 1983). Some assumptions about the upper cut-off frequency is essential for this method because of the small number of terms in the histogram. Following Junod's work Loram[23] developed a new approach in which at first a rapidly convergent function G(T) is generated from $C_v(T)$, and the spectrum $g(\omega)$ is obtained from a least-squares fit to G(T) of a set of functions similarly derived from the Einstein specific heat function. But it required that specific heat measurements of reasonable accuracy must be available up to $\Theta_D/2$. All the methods mentioned above except Montroll's are approximate. Equation (1.7) was not solved directly. There were always some conditions involved which made applying those methods to real systems very difficult. In 1990, Kok[24] proposed a method to solve this problem using a minimization procedure. First he applied the trapezoidal rule to the RHS of equation (1.9). Then one has a set of linear equations in x_k:

$$\sum_{k=1}^{m} a_{jk} x_k = G_j \qquad (j = 1, 2, ..., n) \qquad (2.2)$$

or in matrix form: AX = G, where

$$a_{jk} = \frac{(\hbar\omega_k/kT_j)^2 \, e^{\hbar\omega_k/kT_j}}{(e^{\hbar\omega_k/kT_j} - 1)^2},$$

$$G_j = G(T_j), \qquad x_i = g(\omega_i)\,\Delta\omega,$$

since the specific heat measurements are subject to experimental errors, defining

$$V = AX - G \qquad (2.3)$$

and minimizing V^TV, the phonon density of states can be found by the standard method of steepest descent. A numerical example was presented by Kok. Here we show it in Fig. 2.3.

Recently, as the FFT and signal processing theory have become well developed, one has the possibility to try Montroll's method. N. Chen, Y. Chen et al. [25] have applied the method to several materials with face-centered-cubic structure. Introducing the new variables x and y as

$$e^x = \hbar\omega/k, \qquad e^y = T,$$

then equation (1.6) becomes

$$C(y) = \int_{-\infty}^{\infty} \Phi(y-x)G(x)dx = \Phi(y)*G(y) \tag{2.4}$$

where

$$C(y) = \frac{\hbar}{k^2} e^{-\delta y} C_v(e^y),$$

$$G(x) = e^{(1-\delta)x} g((k/\hbar)\, e^x)$$

and the integral kernel is

$$\Phi(u) = \frac{e^{-(\delta+2)u}\, e^{e^{-u}}}{(e^{e^{-u}} - 1)^2} \tag{2.5}$$

For all of the three functions, $\Phi(u)$, $C(y)$ and $G(x)$, one can carry out Fourier transforms. From equation (2.4), one has

$$G(x) = F^{-1}\{ F[C]/F[\Phi]\} \qquad (2.6)$$

Thus the unknown frequency distribution $g(\omega)$ can be inferred from the specific heat function. Some numerical examples shown in Fig. 2.4 were presented by Chen et al.[25].

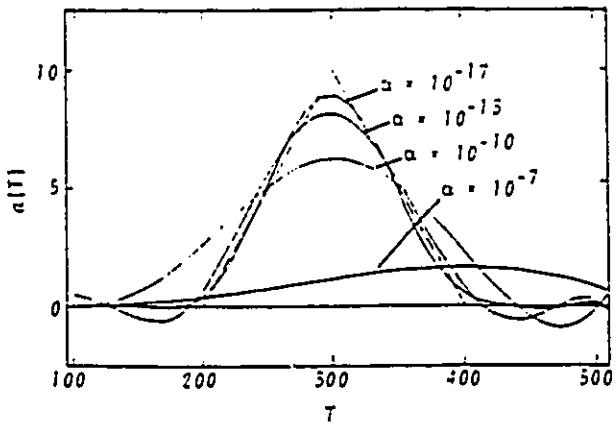

FIG. 1. Regularization reconstructions (solid lines) of a triangular area temperature distribution profile $a(T)$ as a function of temperature T for different regularization parameter α values. The reconstructions approach the ideal profile (dashed line) as α become small.

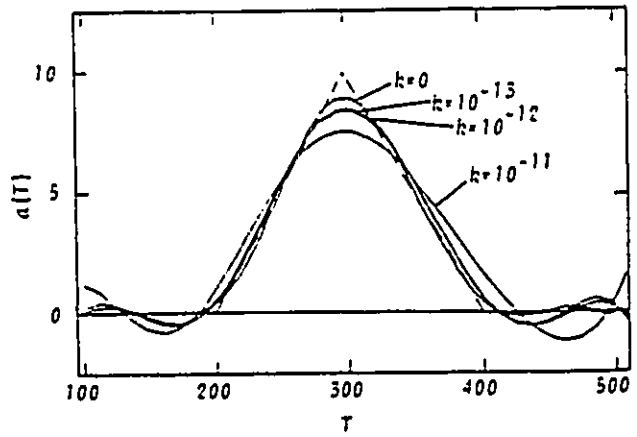

FIG. 3. Regularization reconstructions of the triangular profile $a(T)$ shown in Fig. 1 in presence of additive noise. Here k is a measure of the noise amplitude as defined by (19).

Fig. 2.1 Numerical results for black body radiation problem presented by Sun et. al. based on Tikhonov regularization method.

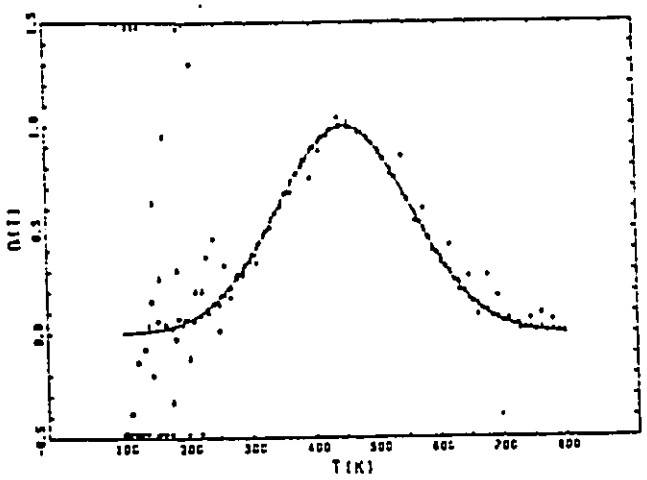

Fig. 4. Calculated temperature distributions along with ideal Gaussian curve.

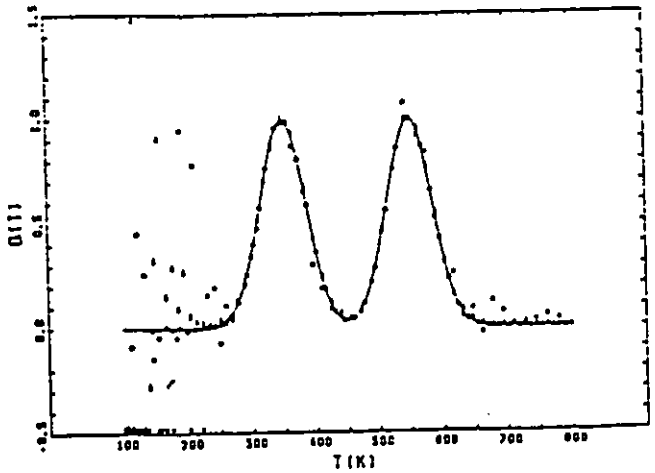

Fig. 7. Calculated temperature distributions along with ideal curve of double Gaussian.

Fig. 2.2 Numerical results for black body radiation problem presented by Chen based on Fourier deconvolution.

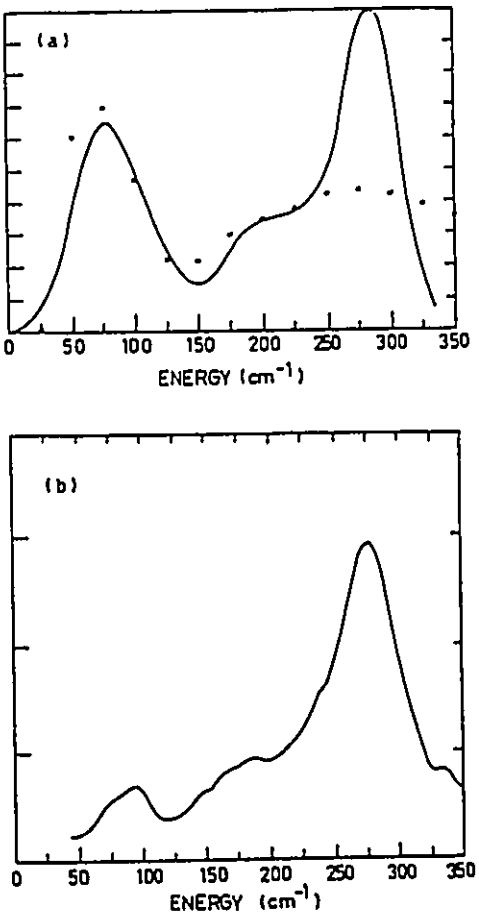

Fig. 1. (a) × Calculated density of states of amorphous germanium; —— Density of states of crystalline Ge is broadened by a convolution with a Gaussian factor of half-width 25 cm $^{-1}$ [8]. (b) —— The reduced Raman spectrum of amorphous Ge from room temperature data [8].

Fig. 2.3 Numerical results for phonon density of states problem presented by Kok using a minimization procedure.

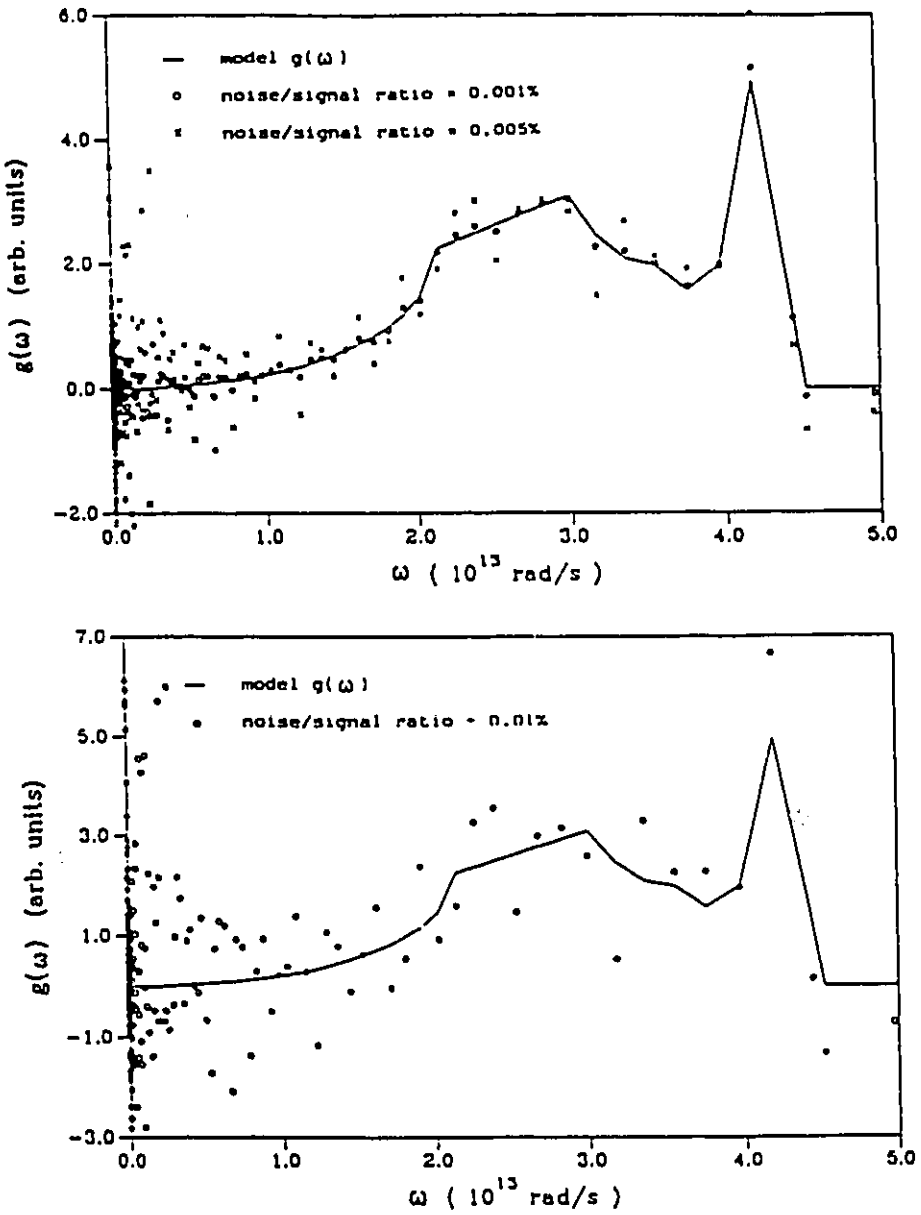

Fig. 5. The calculated frequency distribution $g(\omega)$ from modified $C_v'(T)$ with noise/signal ratio of 0.001%, 0.005% and 0.01%.

Fig. 2.4 Numerical results for phonon density of states problem presented by Chen based on Fourier deconvolution.

CHAPTER THREE

Regularization Method

1. Brief review of the regularization method

The regularization method, as a method to deal with ill-posed problems, was proposed by Tikhonov[1-2] and Phillips[3] in 1963 and 1962, respectively. In Tikhonov's pioneering work, he gave a definition of an ill-posed problem and theoretically developed a regularization method which resulted in the replacement of the ill-posed problem by a well-posed problem. Some theorems were developed to prove that this regularizing method can solve the ill-posed problem with a unique and stable solution. In Phillip's work, he concentrated on the Fredholm integral equation of the first kind which is a kind of ill-posed problem. A numerical algorithm was proposed. Simple numerical examples were also given to show the efficiency of this method. But there was no application to any concrete physics problem. Since then an intensive development of the theory of the method and its application to difficult practical problems has been done.

Based on the work of Tikhonov and Phillips, Pindor, Igalson et al.[26-27] applied the regularization method to the phonon density of states and the electron-phonon interaction in metals. In his work, however, he didn't pay any attention to how the regularization parameter and operator affect the results. Only one example of the application to a phonon density of states problem was given and the result was not very good. Recently, Sun and Jaggard[4] carried out another implementation of the regularization method to solve the inverse black body radiation problem. Some encouraging results were obtained. However only the zero- and first-order regularization operator were used in their work. In the following sections, a simple implementation of the regularization method will be introduced and applied to the inverse black body radiation and phonon density of states problems. Some very good results will be presented.

2. Principle of the regularization method

Consider the Fredholm integral equation:

$$\int_a^b k(x,y)\, f(y)\, dy = g(x) \qquad c \le x \le d \qquad (3.1)$$

As we have seen in Chapter One, this equation is an ill-posed problem. If the matrix approximation which is successfully applied for the solution of a well-posed problem is used, (3.1) can be replaced approximately by the algebraic system:

$$\sum_{i=1}^{N} v_i k_{ji} f_i = g_j \qquad (3.2)$$

where $f_i=f(x_i)$; $g_j=g(x_j)$; $k_{ji}=k(x_j,y_i)$, v_i are weight factors whose values depend on the quadrature formula used.

It is found that as the mesh width decreases, the solutions at first become more accurate, but eventually begin to get worse. How soon the solutions begin to get worse depends on the accuracy of g(x) and the shape of the kernel function k(x,y). It turns out that the roots f_1, f_2, ... f_n of (3.2) do not lead to a continuous curve, but to a curve which makes violent oscillations.

For convenience, define a linear operator

$$K: \quad F \Rightarrow G$$

by

$$(Kf)(x) = \int_a^b k(x,y)f(y)dy \qquad (3.3)$$

Since in practical situations, the data function g(x) is often the output of some measuring process and it is not known accurately, we should state the problem as:

$$(Kf)(x) = g(x)+\varepsilon(x) = \mathfrak{g}(x) \qquad (3.4)$$

where $\varepsilon(x)$ is an arbitrary bounded function.

Here instead of a unique solution of (3.4), we are dealing with a problem which has a family $\mathcal{F}$ of solutions. The problem then is to pick the true solution f out of the family of functions $\mathcal{F}$. To do this, we need more information about the problem than is given in equation (3.4). Usually in practice, function f is a smooth function rather than an oscillating function. Using the condition that f is a reasonably smooth function, Tikhonov proposed a regularization method which can damp out those oscillations and regularize the solution process.

Introducing a regularizing operator L and a parameter α, the problem can be stated as the problem of minimizing the functional

$$\Phi_\alpha(f) = \| Kf - \mathfrak{g} \|^2 + \alpha \| Lf \|^2 \qquad (3.5)$$

over all functions f in the compact set :

$$\{ f: \| Kf - g(x) \| \leq \varepsilon(x) \} \qquad (3.6)$$

$\| Lf \|^2$ is called a stabilizer. The duty of the parameter α is to effect a trade-off between smoothness (large α) and fidelity (small α) in the approximate solution.

Tikhonov[1-2] proved that (3.5) has a unique solution which will be denoted by f_α. Moreover, f_α will converge as $\varepsilon \Rightarrow 0$, uniformly on [a, b], to the solution of the equation

$$\int_a^b k(x,y)\, f(y)\, dy = g(x)$$

provided that α satisfies $C_1\varepsilon < \alpha < C_2\varepsilon$ for positive numbers C_1 and C_2. Since g is not known exactly, i.e, ε is not known, the question then arises as to how to choose the value of α. Up to now, this is still a problem. The proper choice of α depends considerably on the particular problem. Besides the choice of α, another question is how to choose the regularization operator. As mentioned above, we assume that f(y) is a reasonably smooth function. Here the following is chosen:

$$\| Lf \|^2 = \int_a^b \sum_{i=0}^{n} q_i(y) \left(\frac{d^i f(y)}{dy^i}\right)^2 dy \qquad (3.7)$$

It is customary to refer to L as the n^{th}-order regularizing operator. Stabilizers of the form (3.7), where $q_i(y) \geq 0$ for i=0, 1, ... N-1 and $q_N(y) > 0$ will be called stabilizers of n^{th}-order. If all the functions $q_i(y)$ are constants, they will be called stabilizers of n^{th}-order with constant coefficients. Conditions under which this operator exists are examined in [6].

3. Numerical algorithm

In order to solve (3.5) numerically, we introduce the following discretizations: we assume that $\tilde{g}(x)$ is given on N not necessarily equidistant points $x = x_i$, $i = 1, 2, ..., N$ ($c \le x_1 < x_2 < ... < x_n \le d$) with $\tilde{g}(x_i) = g_i$, and we split up the integration interval [a, b] into N subintervals $[y_{j-1}, y_j]$, $j = 1, 2, ..., N$ ($a = y_o < y_1 < ... < y_N = b$). The integrals $(\mathbf{K} f)(x)$ occurring in (3.5) are approximated, for any given $x = x_i$, by using the repeated mid-point rule:

$$(\mathbf{K} f)(x_i) = \int_a^b k(x_i,y)\, f(y)\, dy$$

$$= \sum_{j=1}^{N} \int_{y_{j-1}}^{y_j} k(x_i,y)\, f(y)\, dy$$

$$\approx \sum_{j=1}^{N} k_{ij}\, f_j$$

where

$$k_{ij} = (y_i - y_{j-1})\, k(x_i, \bar{y}_j)$$

$$\bar{y}_j = \frac{1}{2}(y_{j-1} + y_j)$$

and $f_j = f(\bar{y}_j)$ is an (unknown) approximation of f at the point $\bar{y}_j$. After defining $\tilde{f}_j = \tilde{f}_j(\bar{y}_j)$ as an a priori known estimate of f_j,

$$\varepsilon_i = \sum_{j=1}^{N} k_{ij} f_j - g_i, \qquad i=1,2,...,N,$$

and writing

$$Lf = a_0 (f - \bar{f}) + a_1 f' + a_2 f''$$

where, $a_i = 0$ or 1, we replace the continuous problem (3.5) by the discrete problem:

minimize the quadratic functional $\Phi_\alpha(f)$, defined by

$$\Phi_\alpha(f) = \sum_{i=1}^{N} \varepsilon^2_i + \alpha \left\{ a_0 \sum_{j=1}^{N} (f_j - \bar{f}_j)^2 + a_1 \sum_{j=1}^{N-1} (f_{j+1} - f_j)^2 \right.$$
$$\left. + a_2 \sum_{j=2}^{N-1} (f_{j+1} - 2 f_j + f_{j-1})^2 \right\} \qquad (3.8)$$

over all vectors

$$A:[f_1 , f_2 ,..., f_N]^T \in R^N$$

for which

$$\sum_{i=1}^{N} \varepsilon_i^2 \le \varepsilon^2.$$

From the necessary condition

$$\partial \Phi_\alpha / \partial f_j = 0, \quad j=1,2,...,N$$

we find, after some simple calculations, the linear matrix-vector equation:

$$\{K^T K + \alpha(a_0 H_0 + a_1 H_1 + a_2 H_2)\}\, f = K^T g + \alpha a_0 \tilde{f} \qquad (3.9)$$

where

$$g=[g_1,...g_n]^T, \qquad \tilde{f}=[\tilde{f}_1,...,\tilde{f}_N]^T,$$
$$K=(k_{ij}), \qquad K^T=(k_{ji}),$$

$$H_0 = \begin{bmatrix} 1 & & & & \\ & 1 & & 0 & \\ & & \ddots & & \\ & 0 & & 1 & \\ & & & & 1 \end{bmatrix}_{NxN}$$

$$H_1 = \begin{bmatrix} 1 & -1 & & & & \\ -1 & 2 & -1 & & 0 & \\ & -1 & 2 & -1 & & \\ & & \ddots & \ddots & \ddots & \\ & 0 & & -1 & 2 & -1 \\ & & & & -1 & 1 \end{bmatrix}_{NxN}$$

$$H_2 = \begin{bmatrix} 1 & -2 & 1 & & & & & & \\ -2 & 5 & -4 & 1 & & & & 0 & \\ 1 & -4 & 6 & -4 & 1 & & & & \\ & 1 & -4 & 6 & -4 & 1 & & & \\ & & & \ddots & \ddots & \ddots & \ddots & \ddots & \\ & & & & 1 & -4 & 6 & -4 & 1 \\ & 0 & & & & 1 & -4 & 5 & -2 \\ & & & & & & 1 & -2 & 1 \end{bmatrix}_{NxN}$$

The linear symmetric system (3.9) is solved by using the standard IMSL-library routine LEQT2F[28].

4. Applications to the black body radiation problem and the phonon density of states problem

Here, we present some reconstructions of area temperature distributions centered at 450K from the power spectrum function in the frequency band of 10^{10}Hz ~ 2×10^{14}Hz.

The first example uses a Gaussian temperature distribution given by

$$a_1(T) = e^{-\frac{(T-450)^2}{25000}} \qquad 100 \le T \le 800 \tag{3.10}$$

The power spectrum associated with this distribution is given by

$$W_1(\nu) = \frac{2h\nu^3}{c^2} \int_{100}^{800} \frac{a_1(T)\,dT}{e^{h\nu/kT} - 1} \tag{3.11}$$

Fig. 3.1 shows the power spectrum. Then the regularization procedure described in the above section is applied to obtain $a_1(T)$ based on 64 points of the discrete power spectrum data $W(\nu)$. Fig. 3.2 shows the comparison of the ideal $a_1(T)$ values indicated by a solid line and the calculated results of $a_1(T)$ indicated by dots. Here the value of α is

0.00001 and the second-order regularization operator is chosen. As we can see the overall agreement is extremely good.

The second example studied used a triangular temperature distribution

$$a_2(T) = \begin{cases} 0.5 & 100 \le T \le 300 \\ 1 - \frac{1}{300}|T-450| & 300 \le T \le 600 \\ 0.5 & 600 \le T \le 800 \end{cases} \qquad (3.12)$$

Fig. 3.3 shows the same results as Fig. 3.2 for $a_2(T)$. Here $\alpha = 0.00001$. The overall agreement is again very good except for the region near the middle of the curve. A discontinuity exists there.

The third example was a rectangular temperature distribution which provides a more challenging test of the inversion procedure.

$$a_3(T) = \begin{cases} 0.5 & 100 \le T \le 300 \\ 1.0 & 300 \le T \le 600 \\ 0.5 & 600 \le T \le 800 \end{cases} \qquad (3.13)$$

The exact and computed $a_3(T)$ for this case are shown in Fig. 3.4 with $\alpha = 0.00001$. The results are not as good as for the first two examples. It is extremely difficult to reproduce discontinuities.

Example 4 was that of a double Gaussian temperature distribution given by

$$a_4(T) = e^{-\frac{(T-300)^2}{9000}} + e^{-\frac{(T-600)^2}{9000}} \quad 100 \le T \le 800 \qquad (3.14)$$

The results for this case are displayed in Fig. 3.5 with $\alpha = 0.00001$. The overall agreement is very good.

The last example was a double triangular temperature distribution

$$a_5(T) = \begin{cases} 0.5 & 100 \le T \le 200 \\ 1 - \frac{1}{200}|T-450| & 200 \le T \le 400 \\ 0.5 & 400 \le T \le 500 \\ 1 - \frac{1}{200}|T-600| & 500 \le T \le 700 \\ 0.5 & 700 \le T \le 800 \end{cases} \qquad (3.15)$$

Fig. 3.6 shows the comparison with the exact $a_5(T)(\alpha = 0.00001)$. Although the agreement is not very good everywhere, the positions of the two peaks are recovered very well. Comparing the results we obtained here using the regularization method with the other's results shown in Fig. 2.1 and Fig.2.2, it is obvious that our numerical results fit the exact results better than Chen's and Sun's results for the black body radiation problem.

In Fig. 3.7 we show the effects of varying the parameter α for the single Gaussian. For the input data W(v) with low noise, the optimal value of α is found empirically to be 0.00001. For a different model , the optimal value of α will be different. The comparisons of the reconstructions using different order regularization

operators for the Gaussian case are showed in Fig. 3.8. It is obvious that using the second-order operator is much better than the zero-order for this case. The reconstructions shown in Fig. 3.9 uses an exact discrete power spectrum W(ν) corrupted by increasing amounts of additive noise as given by

$$W'(\nu) = W(\nu) + k\, R(\nu)\, W(\nu) \qquad (3.16)$$

where R(ν) are random numbers uniformly distributed between -1 and 1, k is a constant which is called noise/signal ratio (n/s) and W'(ν) is the corrupted version of W(ν). Once again the agreement is satisfactory as long as the noise is not too large. Empirically, when the noise increases, the regularization parameter α should be increased.

Now, let us see some reconstructions of the phonon density of states. Here the circular frequency range is from 0 ~ 5×10^{13}rad/s. The first example is a very simple phonon density distribution shown in Fig. 3.10. The corresponding specific heat of lattice vibration is calculated based on the g(ω) of Fig. 3.10 by using the equation:

$$C_v(T) = N_0\, k \int_0^{\infty} \frac{(\hbar\omega/kT)^2 e^{\hbar\omega/kT}}{(e^{\hbar\omega/kT} - 1)^2} g(\omega)\, d\omega \qquad (3.17)$$

Fig. 3.11 shows the above specific heat. Next the regularization procedure is used to obtain g(ω) based on the data of the specific heat. The comparison of the exact g(ω) and

the reconstruction of the $g(\omega)$ is shown in Fig. 3.12, here α=0.00001, L=2. The overall agreement is excellent.

We next considered some materials with face-centered-cubic structure, such as Cu, Al, and Pb. Their frequency distributions $g(\omega)$ from experiments[25] are very similar and are shown in Fig. 3.13. In this study, a simplified frequency distribution $g(\omega)$ with six different functions given by

$$g(\omega) = \begin{cases} \omega^3/6 & 0 \le \omega \le 2 \\ 2\omega/3 & 2 \le \omega \le 3 \\ 6 - 4\omega/3 & 3.0 \le \omega \le 3.6 \\ \omega - 2.4 & 3.6 \le \omega \le 3.8 \\ 4\omega - 13.8 & 3.8 \le \omega \le 4.2 \\ 34.5 - 7.5\omega & 4.2 \le \omega \le 4.5 \end{cases} \qquad (3.18)$$

is taken as a model for these materials, as shown in Fig. 3.14. The calculated specific heat $C_v(\iota)$ based on this data is very similar to the one shown in Fig. 3.11. The reconstruction of $g(\omega)$ is shown in Fig. 3.15. We can see that the low frequency part has been reconstructed very well. Because there are several discontinuities and the curve is not very smooth in the high frequency part, it is very difficult to reconstruct the high frequency part although the zero-order regularization operator is used.

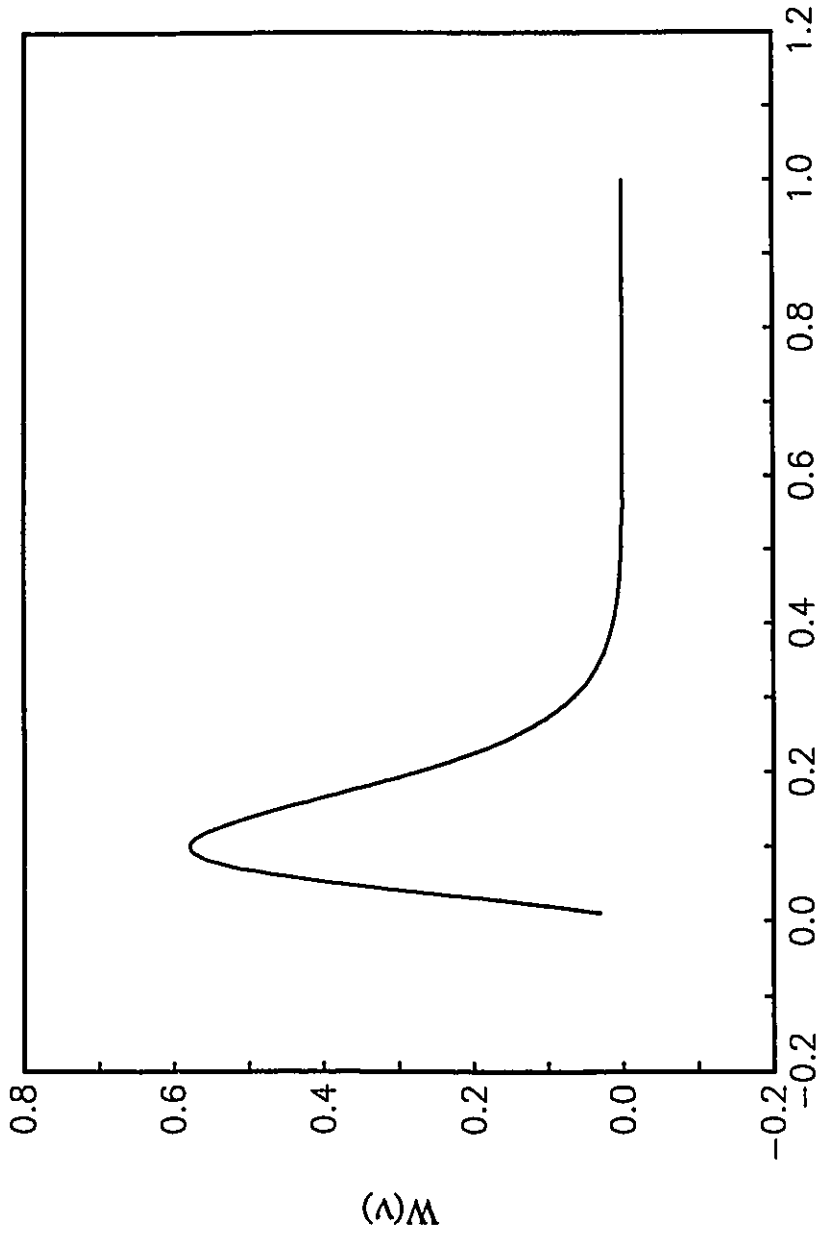

Fig. 3.1 Radiated power spectrum for the Gaussian temperature distribution.

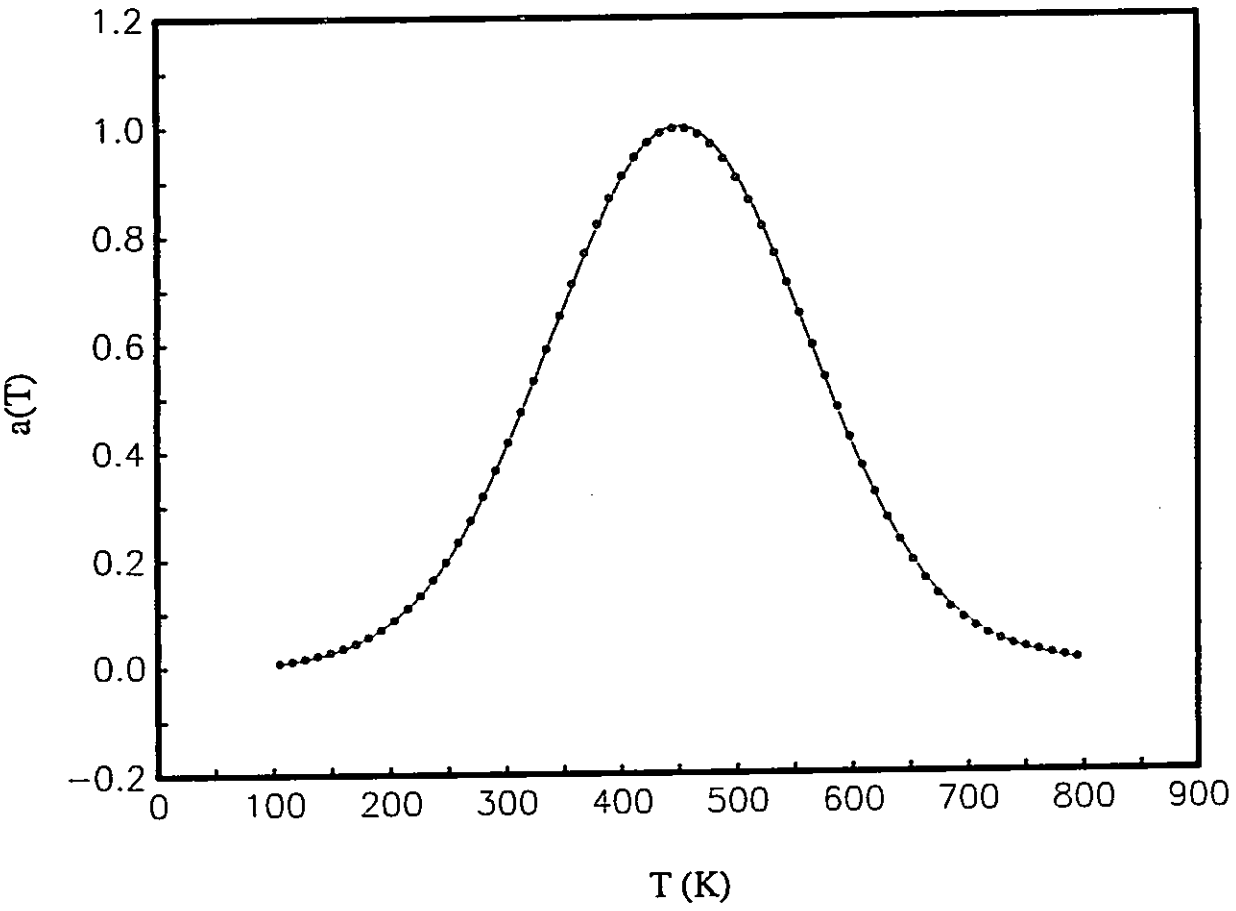

Fig. 3.2 Exact and computed temperature distributions for the Gaussian distribution.

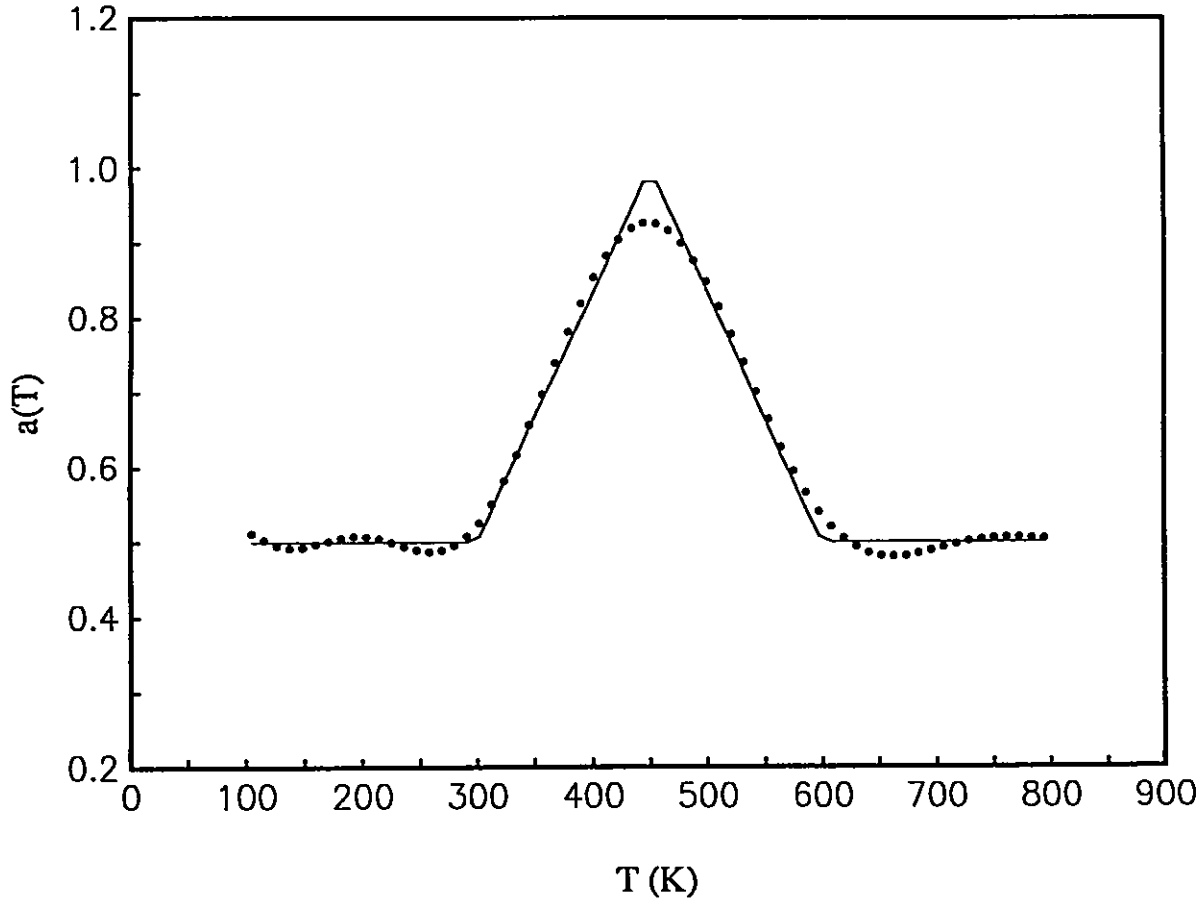

Fig. 3.3 Exact and computed temperature distributions for the triangular distribution.

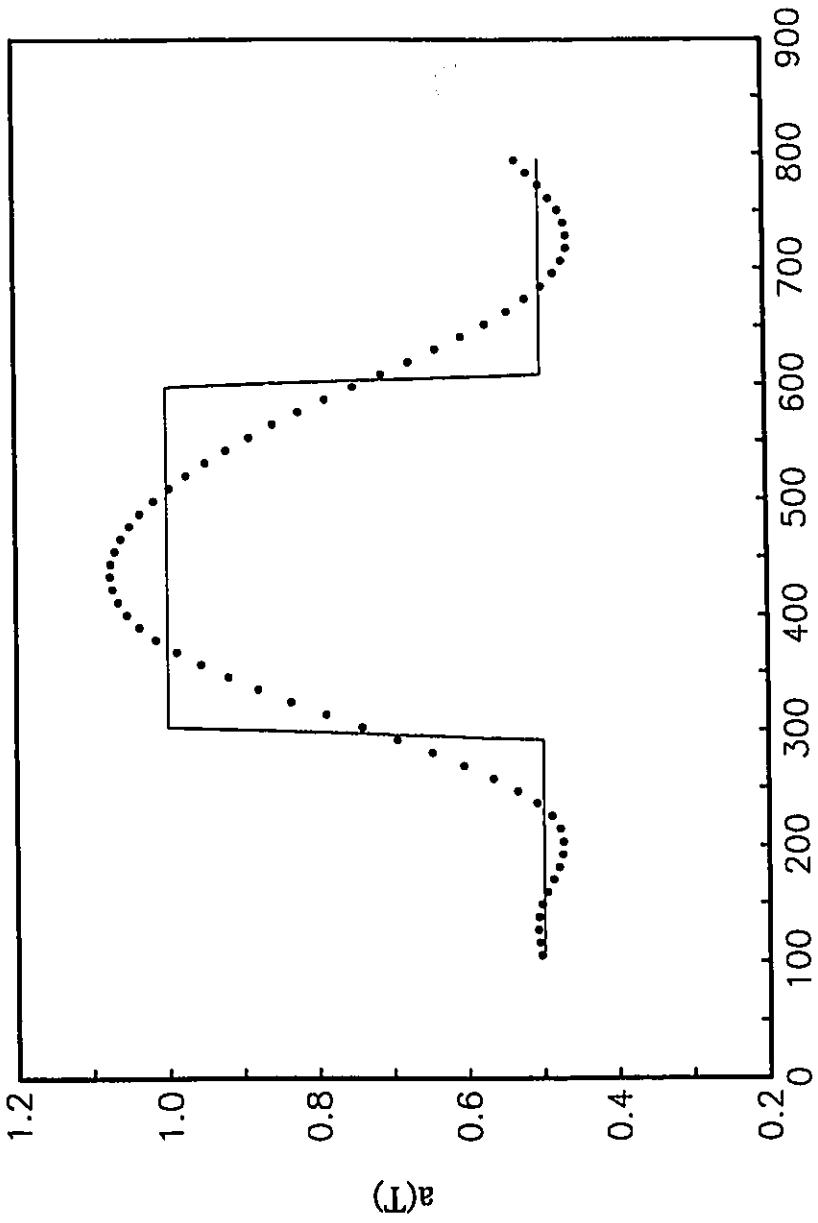

Fig. 3.4 Exact and computed temperature distributions for the rectangular distribution.

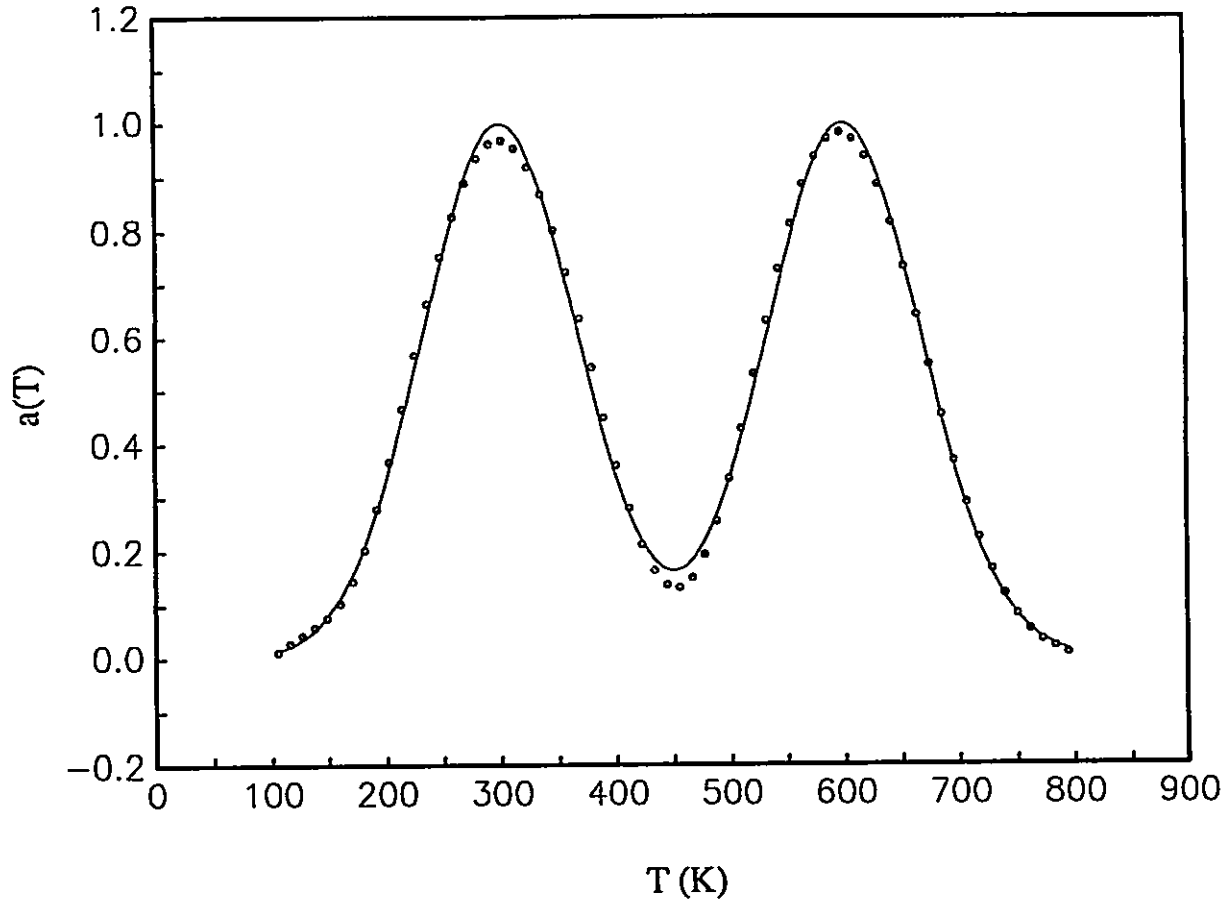

Fig. 3.5 Exact and computed temperature distributions for the double Gaussian distribution.

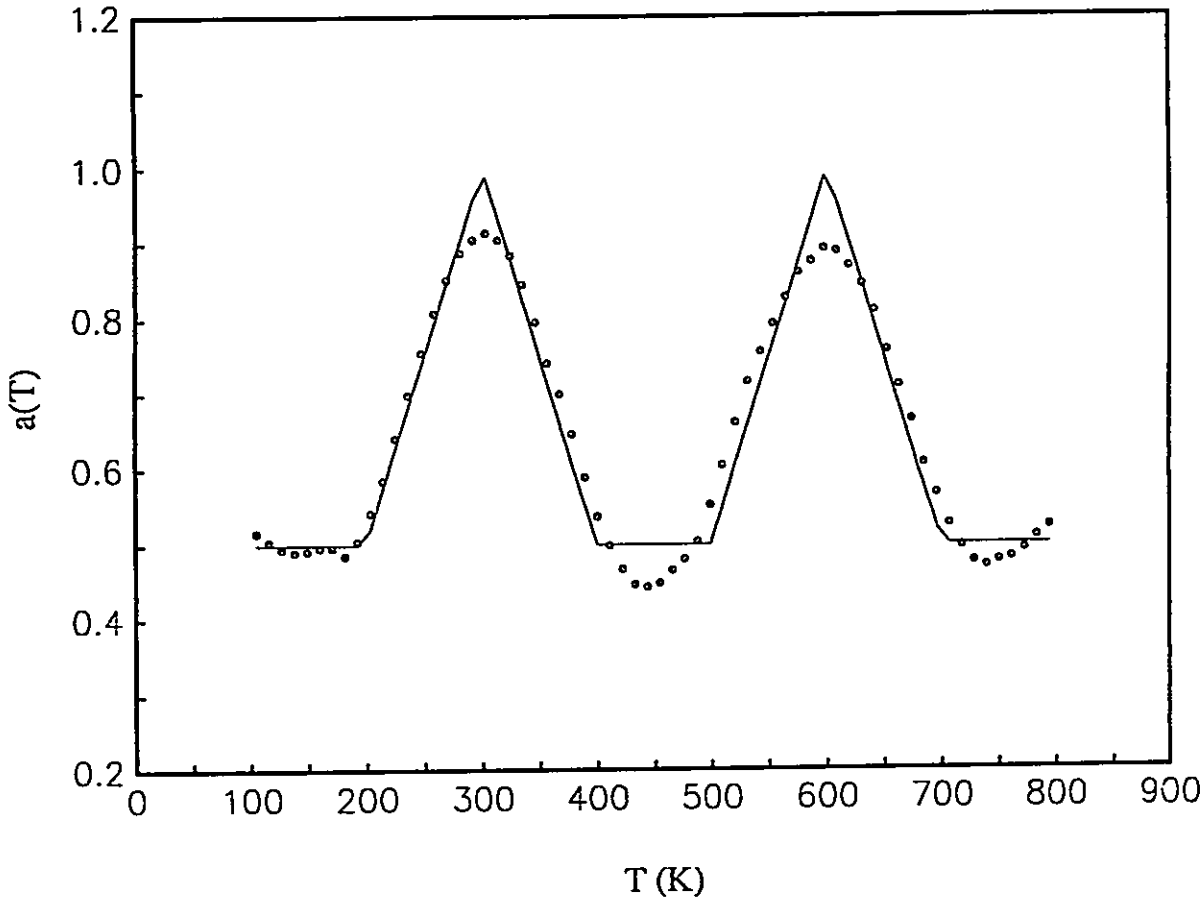

Fig. 3.6 Exact and computed temperature distributions for the double triangular distribution.

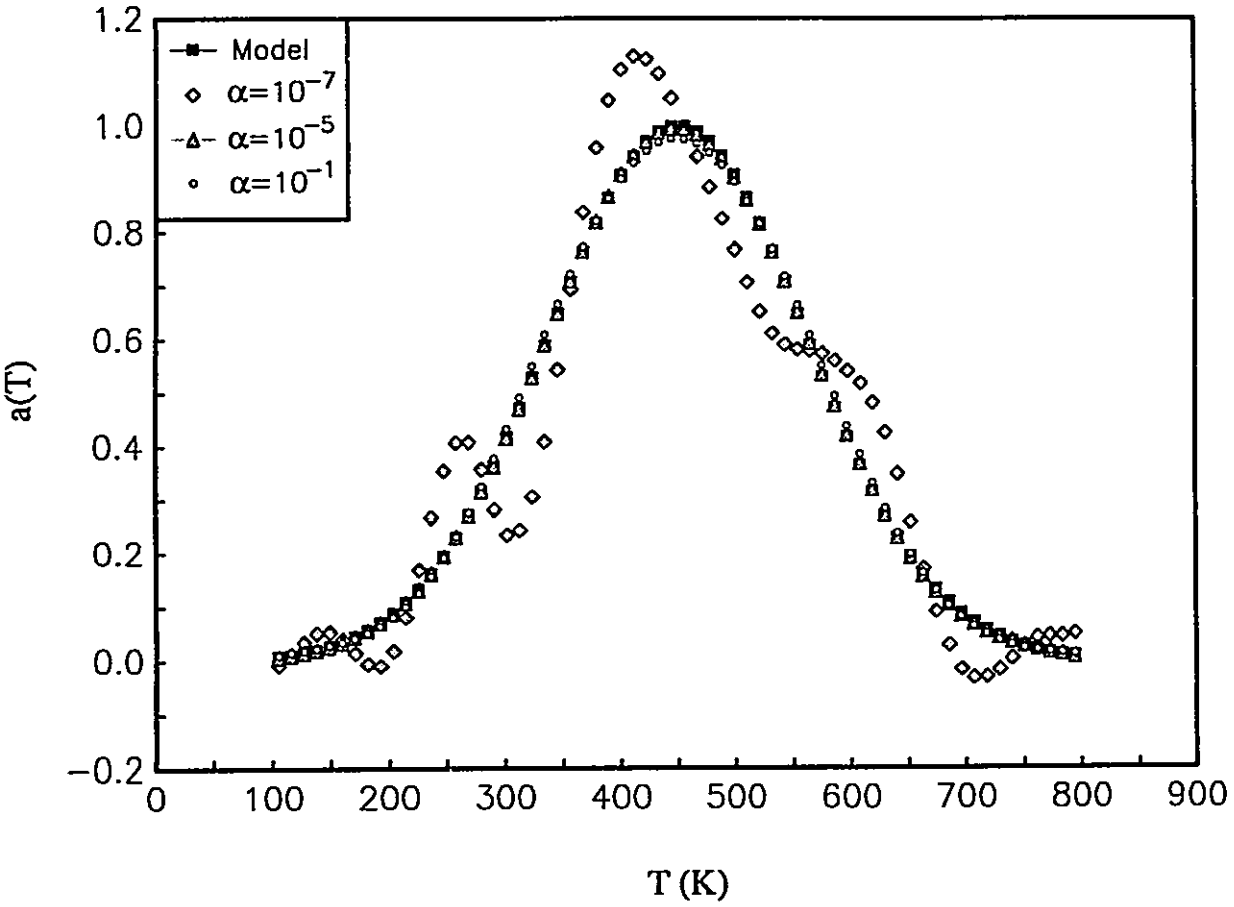

Fig. 3.7 Exact and computed temperature distributions for the Gaussian distribution with different regularization parameters.

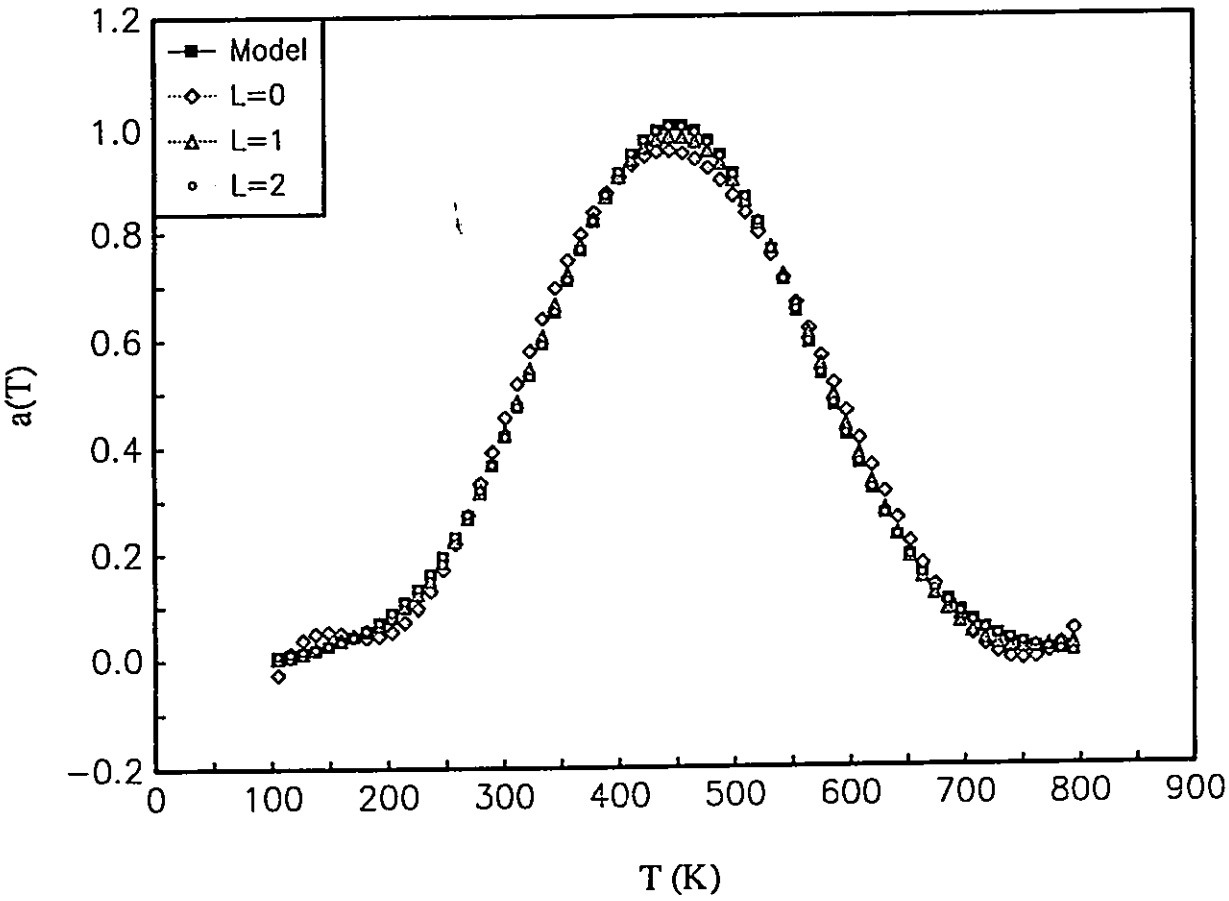

Fig. 3.8 Exact and computed temperature distributions for the Gaussian distribution with different regularization operators.

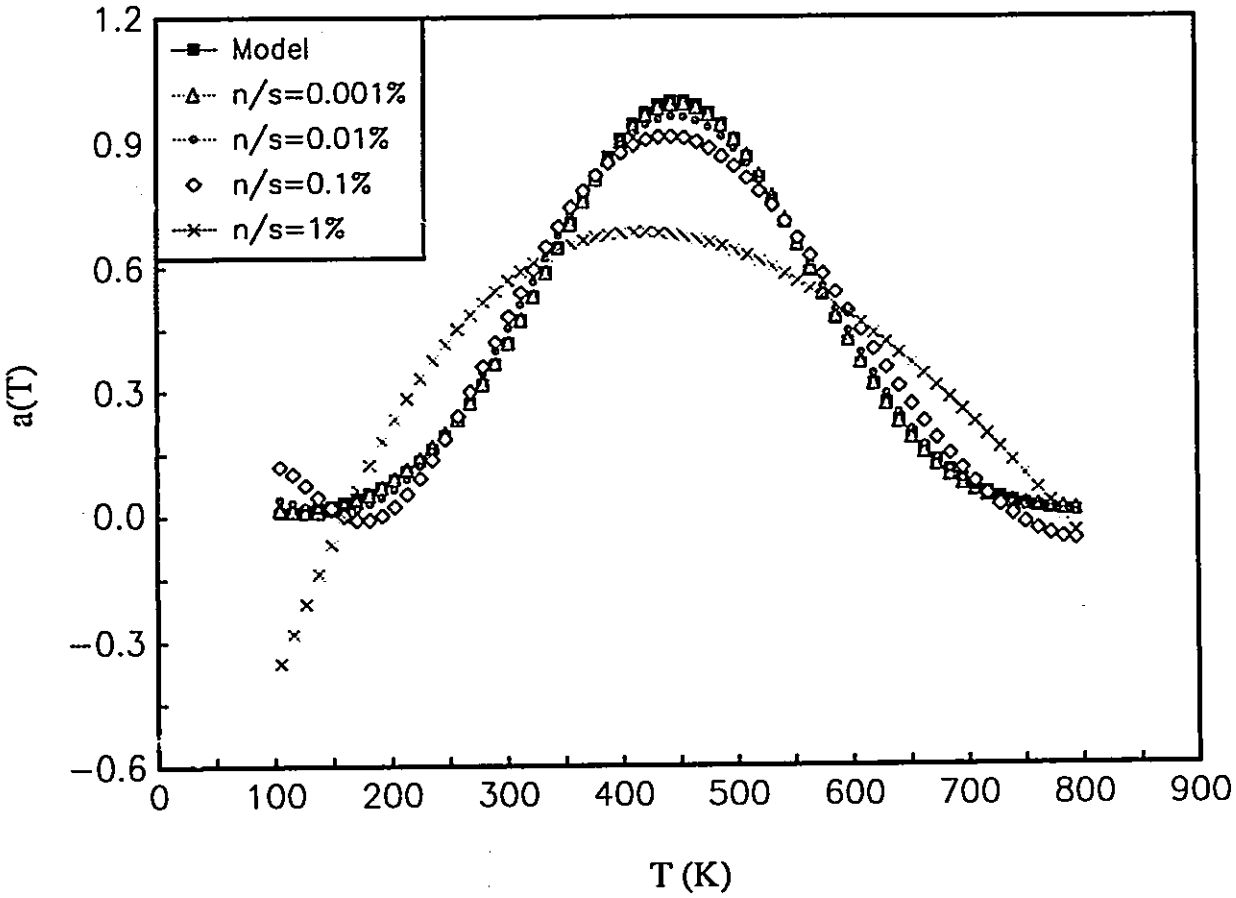

Fig. 3.9 Exact and computed temperature distributions for the Gaussian distribution with different noise-signal ratios in input data.

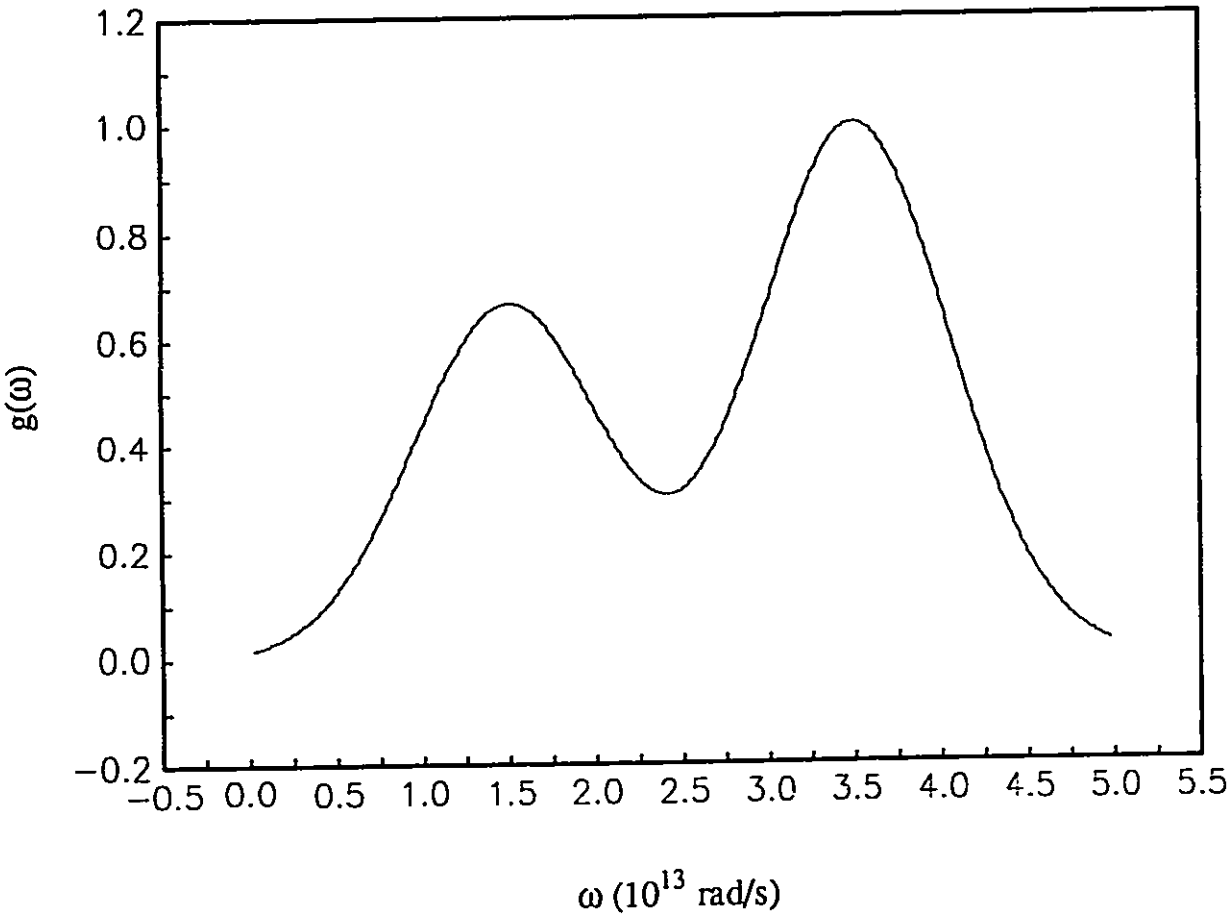

Fig. 3.10 A simple model of the phonon density of states distribution g(ω).

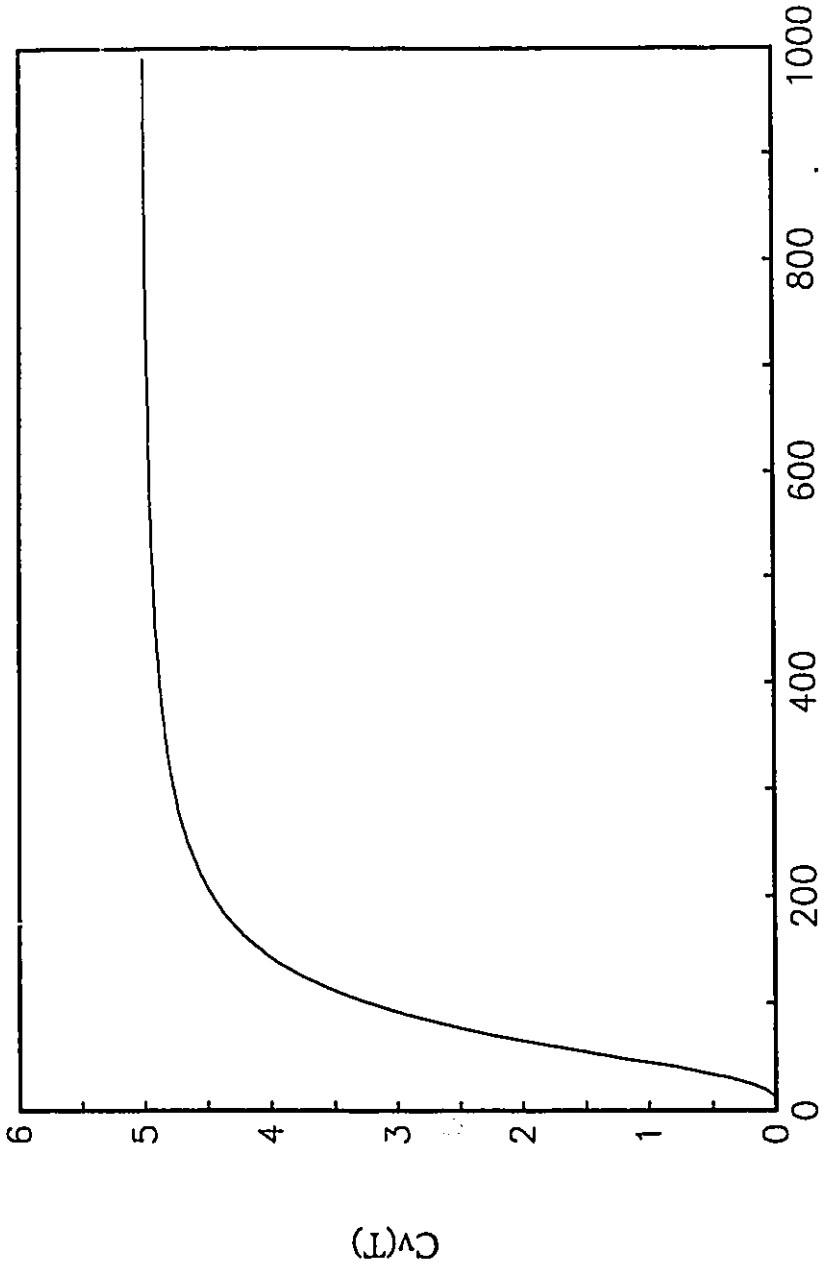

Fig. 3.11 The calculated specific heat Cv(T) based on the data of the model $g(\omega)$ in Fig. 3.10.

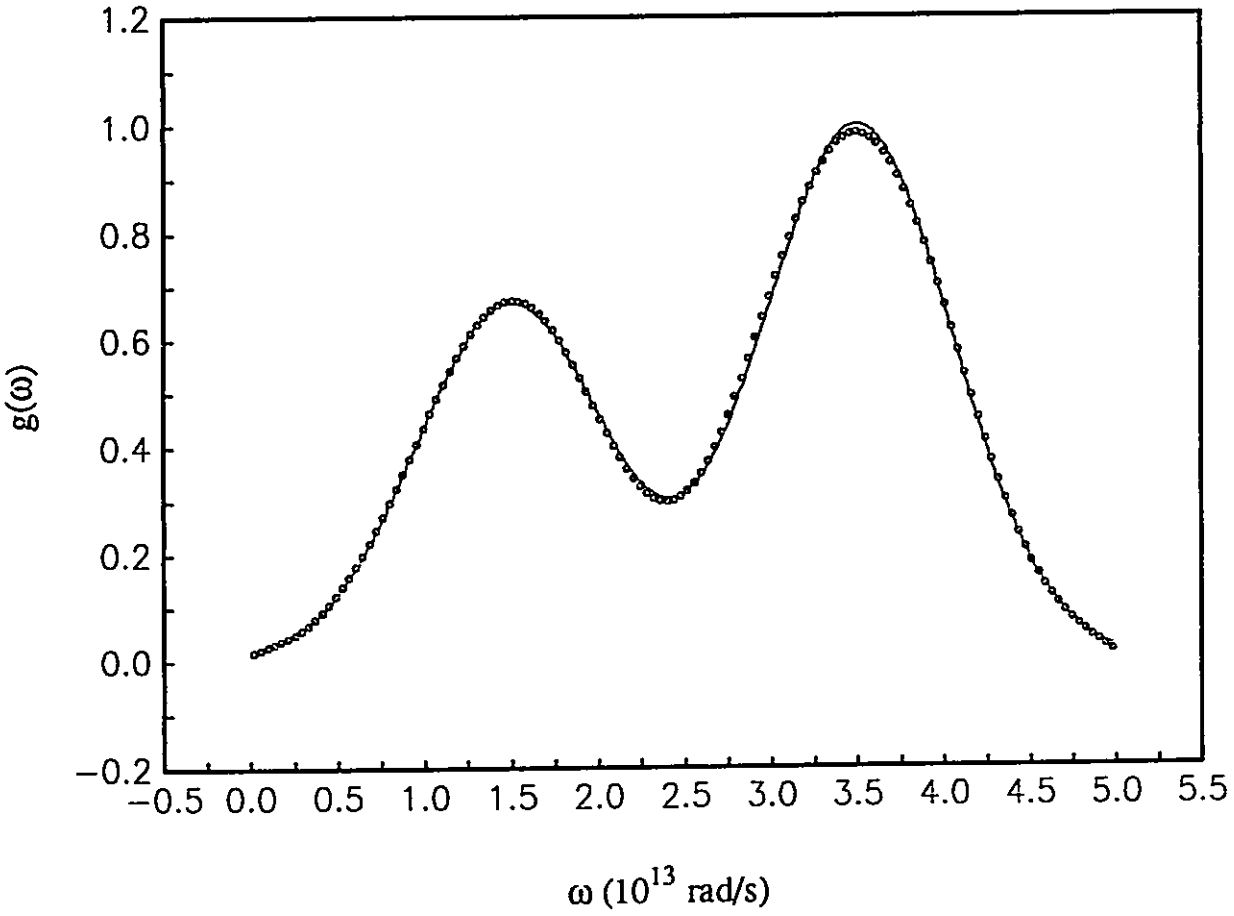

Fig. 3.12 Exact and computed phonon density of states distributions.

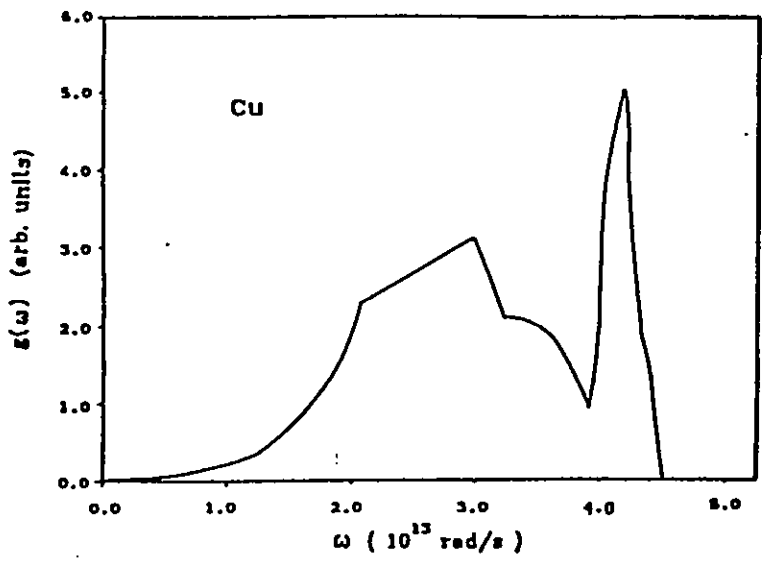

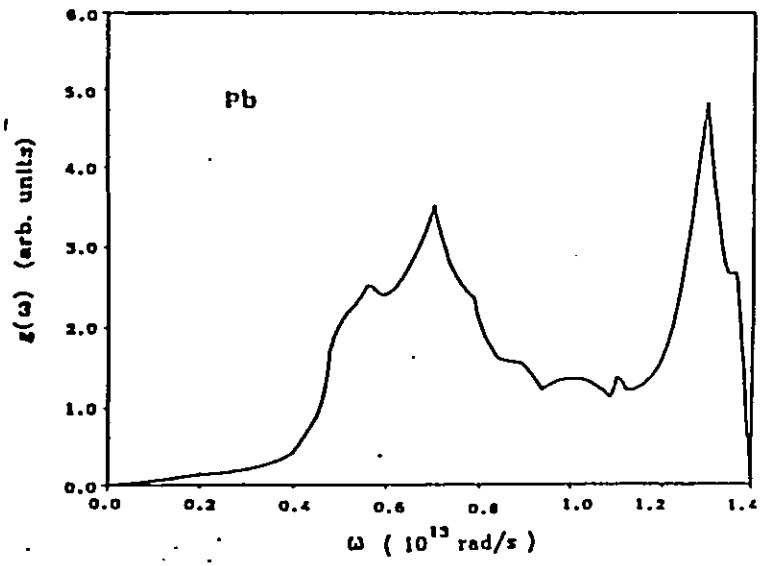

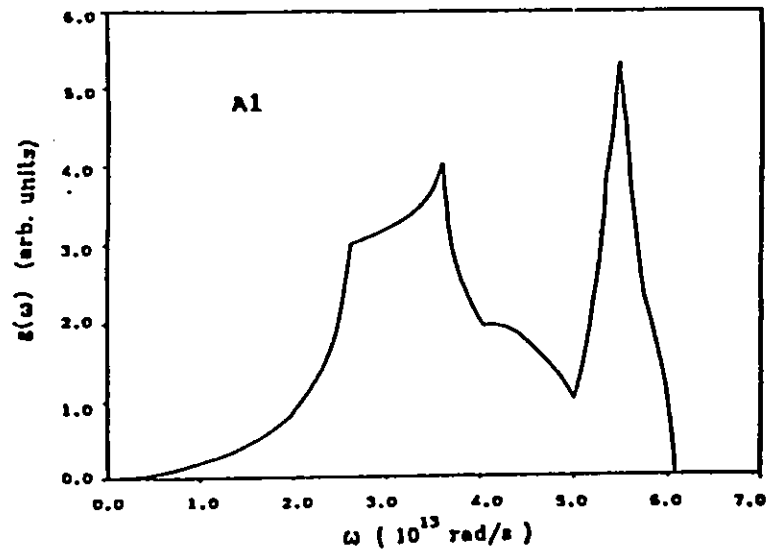

Fig. 3.13 The phonon density of states distribution $g(\omega)$ from experiment for Cu, Al and Pb.

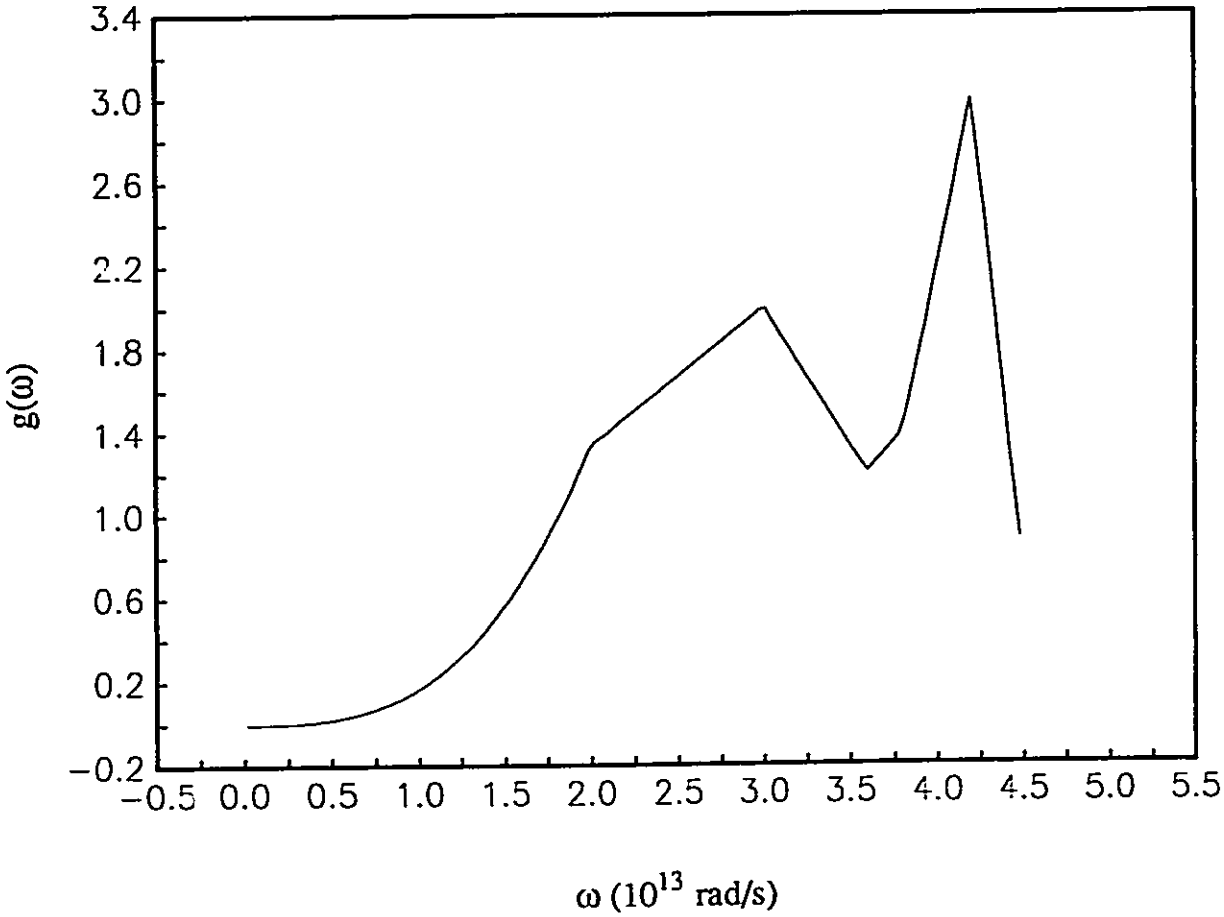

Fig. 3.14 Phonon density of states distribution model for the materials with face-centered-cubic structure.

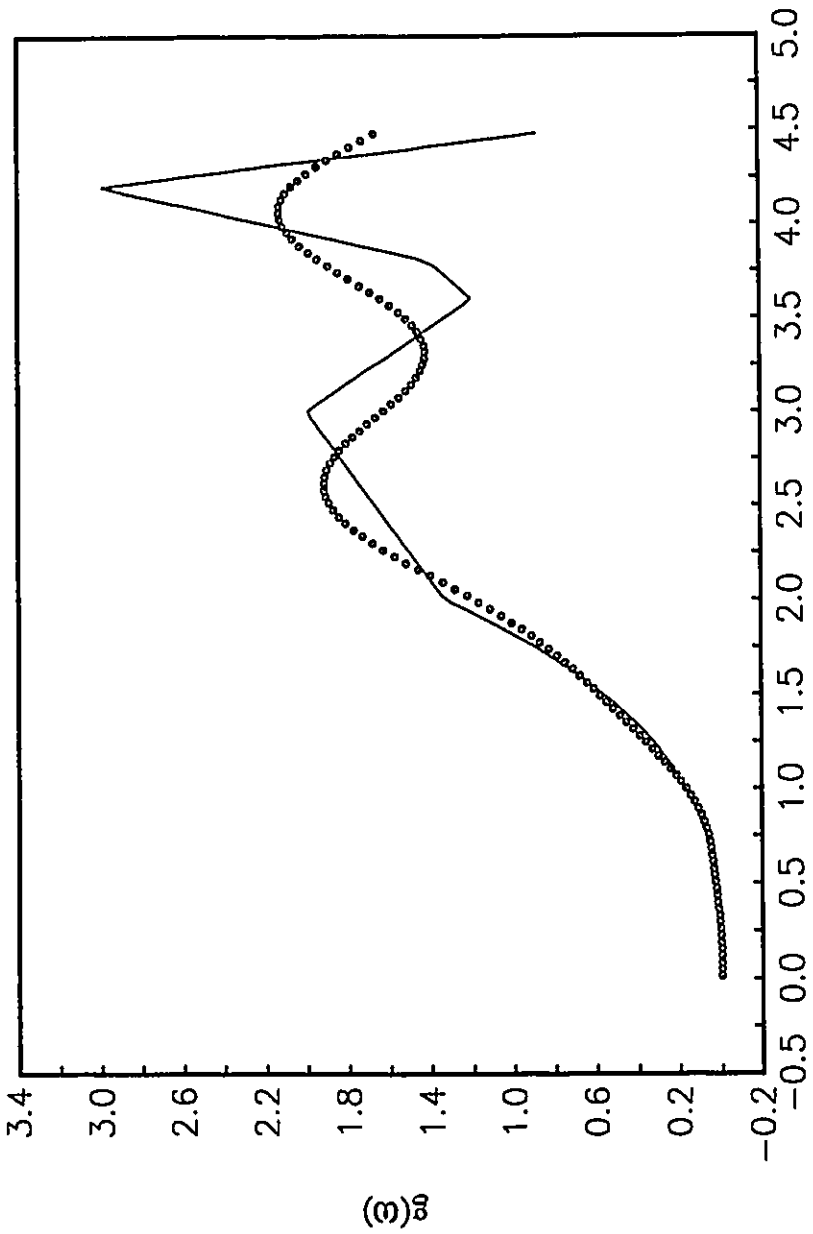

Fig. 3.15 Exact and computed phonon density of states distributions.

CHAPTER FOUR

Maximum Entropy Method

1. Brief review of the maximum entropy method

The concept of information entropy was first introduced by Shannon[5] to describe the information content in a signal. Following his work, Jaynes[29-30] proposed the principle of maximum entropy as a method of statistical inference and applied it to problems of statistical mechanics. Since the time of these introductions, this principle has found application in a wide variety of fields, such as digital signal and digital image processing, geophysical data analysis[31] etc. Recently the maximum entropy method has proven to be a very useful and effective tool to obtain approximate solutions to certain classes of differential[32-35] and integral equations[36-38] encountered in theoretical physics. For example: Inguva and Baker-Jarvis[32] have studied the generalized inverse scattering method in the context of maximum entropy methods. Baker-Jarvis[33] solved a class of linear boundary value problems using various

moments of the differential equation as constraints when maximizing the entropy. Meanwhile Mead and Papanicolaou[36] developed a procedure to solve the moment problem with the maximum entropy technique and established necessary and sufficient conditions for the existence of a maximum-entropy solution. Of particular importance to the present work is a paper by Mead[37] on approximate solutions of Fredholm integral equations by the maximum entropy method in which the general Fredholm integral equation is converted to a generalized moment problem whose approximate solution by maximum entropy methods has been implemented in [36]. But he didn't apply this approach to any concrete physics problem. In the following we will demonstrate the applicability of the maximum entropy method as an alternative procedure for the determination of the temperature distribution of a black body from the measured power spectrum and the phonon density of states from the measured specific heat. The principle of the method will be described and the numerical implementation for solving these two inverse problems based on this method will be given in detail. Some numerical results will be given to show the efficiency of the method.

2. Principle of the maximum entropy method

In order to introduce the maximum entropy method, we start with the statement of the classical moment problem, where a positive density P(x) or a probability distribution function (pdf) is sought from a knowledge of its power moments or power expectation value:

$$\int_a^b x^n P(x)\, dx = \mu_n \ , \qquad n= 0, 1, 2, ..., N \qquad (4.1)$$

In practice, only a finite number of moments are known. Hence a unique reconstruction of P(x) is impossible as there exits an infinite variety of functions having the same first N+1 moments. This problem of the determination of the density or pdf in cases where little or no information is available, is as old as the theory of probability. Laplace's "Principle of insufficient reason" was an attempt to supply a criterion of choice, in which one said that two events are to be assigned equal probabilities if there is no reason to think otherwise. Hence our problem is to find a density or a pdf which avoids bias and agrees with whatever information is given. Shannon's[5] maximum entropy theory offers a definite procedure for us to determine the best choice of density function P(x).

The entropy of a pdf is defined as follows:

$$H(P) = -\int P(x)\, \ln P(x) dx \qquad (4.2)$$

This entropy function H(P) measures in a unique way the amount of uncertainty represented by the pdf P(x). It has been proven that the pdf P(x) which has maximum entropy is the pdf which avoids bias [5]. For our problem because we don't have any further information about the P(x) except equation (4.1), according to Laplace's "principle of insufficient reason" we must use the density or the pdf P(x) which has maximum entropy subject to the constraint that the first N + 1 moments be equal to the true moments μ_n , n= 0, 1, 2, ..., N. This is accomplished by introducing appropriate Lagrange multipliers. We seek maximization of the entropy functional S=S(P) defined by,

$$S = -\int_a^b [P(x)\ \ln P(x) - P(x)]\ dx + \sum_{n=0}^{N} \lambda_n\ [\ \mu_n - \int_a^b x^n\ P(x)\ dx] \qquad (4.3)$$

Functional variation with respect to the unknown density P(x) yields :

$$\frac{\delta S}{\delta P(x)} = 0 \qquad => \qquad P_N\ (x) = \exp(-\lambda_o - \sum_{n=1}^{N} \lambda_n\ x^n) \qquad (4.4)$$

which is supplemented by the condition that the first N + 1 moments are given by μ_n :

$$\int_a^b x^n\ P(x)\ dx = \mu_n\ , \qquad n= 0, 1, 2, ..., N \qquad (4.5)$$

Suppose that P(x) is normalized, i.e.

$$\int_a^b P(x)\ dx = 1 \qquad (4.6)$$

so that we have :

$$\int_a^b P_N(x)\ dx = \int_a^b \exp[\ -\lambda_o - \sum_{n=1}^{N} \lambda_n\ x^n]\ dx = 1 \qquad (4.7)$$

We can then express λ_o in terms of the remaining Lagrange multipliers,

$$e^{\lambda_o} = \int_a^b \exp[- \sum_{n=1}^{N} \lambda_n x^n] \, dx \equiv Z \qquad (4.8)$$

Combining equations (4.4), (4.5) with (4.8) yields :

$$\begin{cases} \langle x^n \rangle = \mu_n \\ \\ \langle x^n \rangle = \dfrac{\int_a^b x^n \exp[-\sum_{n=1}^{N} \lambda_n x^n] \, dx}{\int_a^b \exp[-\sum_{n=1}^{N} \lambda_n x^n] \, dx} \end{cases} \qquad n = 1, 2, \ldots N \qquad (4.9)$$

The problem of how to solve equation (4.9) to find the λ's will be discussed later.

If the powers of x, x^n , n = 0, 1, 2, ..., N, in (4.1) are replaced with a sequence of functions $G_n(x)$, we would get a generalized moment problem,

$$\int_a^b G_n(x)P(x) \, dx = \mu_n \qquad n=1, 2, 3,.... \qquad (4.10)$$

Here again we assume that

$$\int_a^b P(x)\,dx = 1$$

It then follows logically that,

$$P_N(x) = \exp\left[-\lambda_0 - \sum_{n=1}^{N} \lambda_n G_n(x) \right] \qquad (4.11)$$

$$\begin{cases} \langle G_n(x) \rangle = \mu_n \\ \\ \langle G_n(x) \rangle = \dfrac{\int_a^b G_n(x) \exp[-\sum_{n=1}^{N} \lambda_n G_n(x)]\,dx}{\int_a^b \exp[-\sum_{n=1}^{N} \lambda_n G_n(x)]\,dx} \end{cases} \quad n = 1, 2, \ldots N \quad (4.12)$$

Now , let's consider a general Fredholm equation of the first kind :

$$g(x) = \int_a^b f(y)\, k(x,y)\, dy \qquad c \le x \le d \qquad (4.13)$$

where g(x) and k(x,y) are known. Assuming that f(y) is normalized as before, we can convert (4.13) into an equivalent generalized moment problem [37].

Introducing a linearly independent set of functions $M_n(x)$ with n = 1, 2, ... N, multiplying both sides of (4.13) by $M_n(x)$ and then integrating both sides of this equation with respect to x over the range (c, d) gives a new set of equations as follows:

$$\mu_n = \int_a^b f(y)\, G_n(y)\, dy \qquad n=1, 2, \ldots N \tag{4.14}$$

where

$$\begin{cases} \mu_n = \int_c^d M_n(x)\, g(x)\, dx \\ \\ G_n(y) = \int_c^d M_n(x)\, K(x,y)\, dx \end{cases} \qquad n = 1, 2, \ldots N \tag{4.15}$$

Equation (4.14) is just a generalized moment problem.

3. Numerical algorithm

Considering the system of equations (4.9), it is obvious that an analytical solution is impossible except for the simple case N=1. For numerical as well as theoretical purposes, let's introduce a potential $\Gamma = \Gamma(\lambda_1 , \lambda_2 , \ldots , \lambda_N)$ through the Legendre transformation.

$$\Gamma = \ln Z + \sum_{n=1}^{N} \mu_n \lambda_n \qquad (4.16)$$

Stationary points of this potential are solutions to the system of equations (4.9) [36].

$$\frac{\partial \Gamma}{\partial \lambda_n} = 0 \quad => \qquad \langle x_n \rangle = \mu_n \quad n = 1, 2, \ldots , N \qquad (4.17)$$

It has been shown by Mead and Papannicolaou[36] that Γ is a convex function and that a necessary and sufficient condition for the potential Γ to have a unique absolute minimum at some finite $\lambda_1 , \lambda_2 , \ldots , \lambda_N$ for any N, is that the moment sequence $\{\mu_n , n = 0, 1, \cdots\cdots\}$ should be completely monotonic. Thus it is quite easy to make μ_n satisfy this condition by properly introducing a linearly independent set of functions $M_n(x)$. Finally a minimization program can be used to search for a minimum of Γ starting from some user supplied initial λ's. In this study a local minimization program called MINUIT[39] is used to do the minimization.

4. Applications to the black body radiation problem and the phonon density of states problem

First the foregoing is applied to a few examples in the inverse black body radiation problem. In the following , we have chosen the set of transformation functions to be

$$M_n(v) = e^{nv} \qquad n=1, 2, ..., N \qquad (4.18)$$

Here N is chosen to be 8. Theoretically the larger the number of parameters, the better fit will come out. But numerically the process of determining the minimum becomes increasingly difficult with the increasing number of parameters and more CPU time will be taken. In this work, several different numbers have been tested. When the number of parameters increase from 4 to 8 step by step , the results have been improved notably, but after that increasing the number of parameters doesn't help much.

The first example studied used a Gaussian temperature distribution given by

$$a_1(T) = e^{-\frac{(T-450)^2}{25000}} \qquad 100 \leq T \leq 800 \qquad (4.19)$$

Application of the maximum-entropy method to this distribution resulted in the temperature distribution a(T) as shown in Fig. 4.1. Here the agreement is successful.

The second example was that of a triangular temperature distribution,

$$a_2(T) = \begin{cases} 0.5 & 100 \le T \le 300 \\ 1 - \frac{1}{300}|T-450| & 300 \le T \le 600 \\ 0.5 & 600 \le T \le 800 \end{cases} \qquad (4.20)$$

The exact and computed temperature distributions are displayed in Fig. 4.2. Here the overall agreement is quite good except for the regions near discontinuities.

Example 3 is that of a rectangular temperature case:

$$a_3(T) = \begin{cases} 0.5 & 100 \le T \le 300 \\ 1.0 & 300 \le T \le 600 \\ 0.5 & 600 \le T \le 800 \end{cases} \qquad (4.21)$$

The computed results are shown in Fig. 4.3. The results are not as good as for the first two examples. It is very difficult to reconstruct the discontinuity. The final example is the double Gaussian temperature distribution given by

$$a_4(T) = e^{-\frac{(T-300)^2}{9000}} + e^{-\frac{(T-600)^2}{9000}} \quad 100 \le T \le 800 \qquad (4.22)$$

The computed results in Fig. 4.4 show some disagreement, in the sense that the points at which the temperature distributions are maximum are not reproduced, but have been shifted a little bit. Here again, the results we obtained for the black body radiation problem using maximum entropy method are comparable with or even better than Chen's and Sun's results shown in Fig. 2.1 and 2.2. However there is one thing we need to point

out. The maximum entropy procedure presented here is based on the assumption that there is no noise involved in the input data. If the input data are corrupted with noise, the procedure has to be modified from its beginning. A lot of work will be needed. This will be our next work.

This procedure has also been applied to the phonon density of states problem. The first example is the distribution shown in Fig. 3.10. The comparison of the exact $g(\omega)$ and the reconstruction of the $g(\omega)$ using the maximum entropy procedure is shown in Fig. 4.5. This reconstruction is not as good as the one obtained by using the regularization method, but the overall agreement is quite good. The second example is the distribution shown in Fig. 3.14 for some materials with face-centered-cubic structure. The corresponding results obtained using maximum entropy method are shown in Fig. 4.6. Here only the low frequency part has been successfully reconstructed.

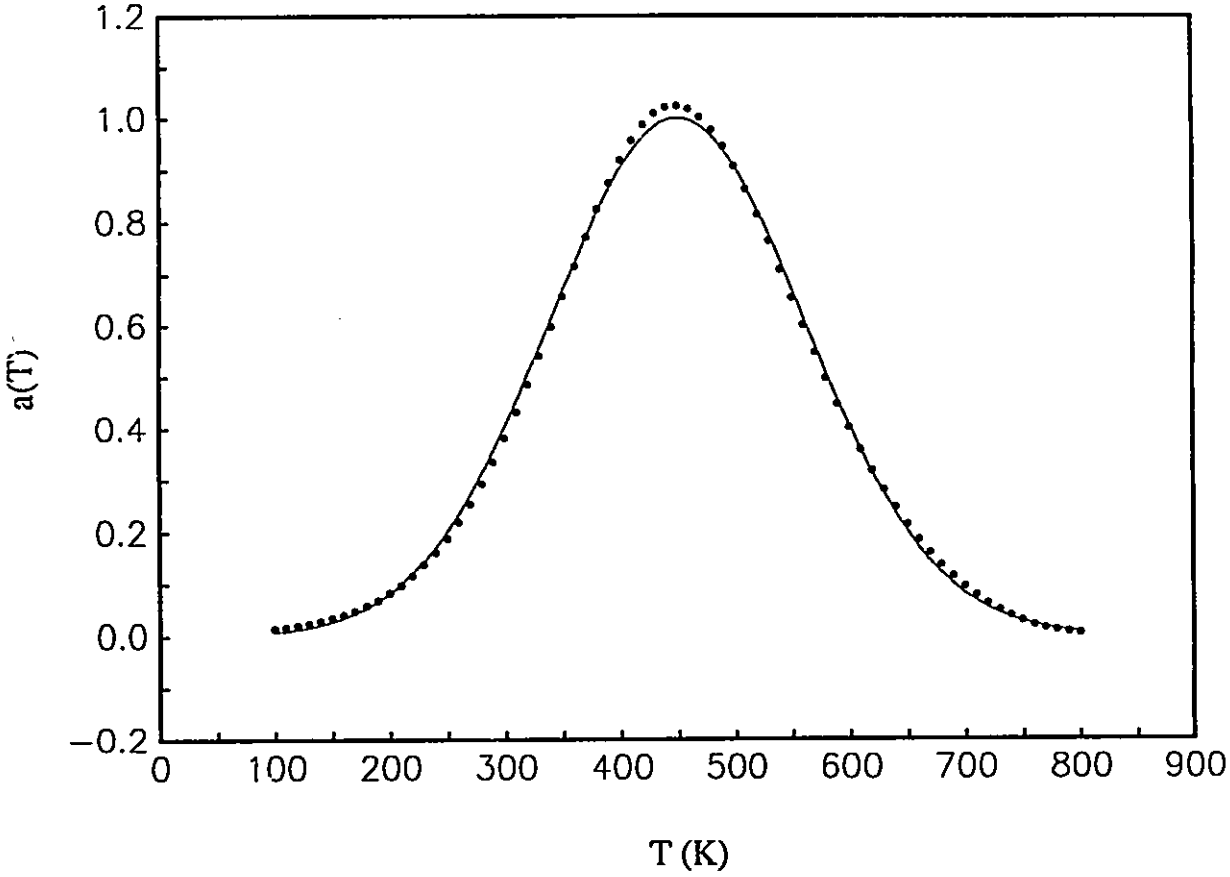

Fig. 4.1 Exact and computed temperature distributions for the Gaussion distribution.

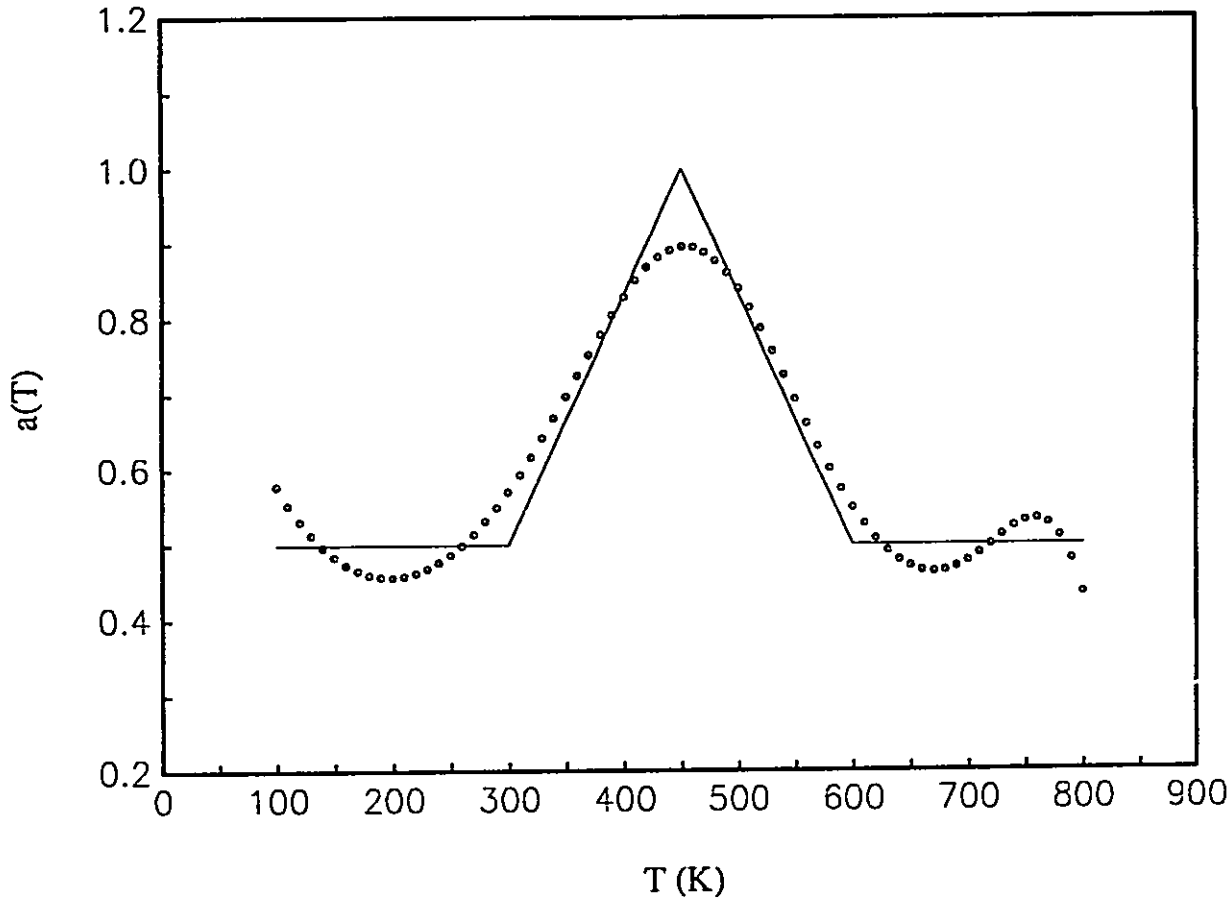

Fig. 4.2 Exact and computed temperature distributions for the triangular distribution.

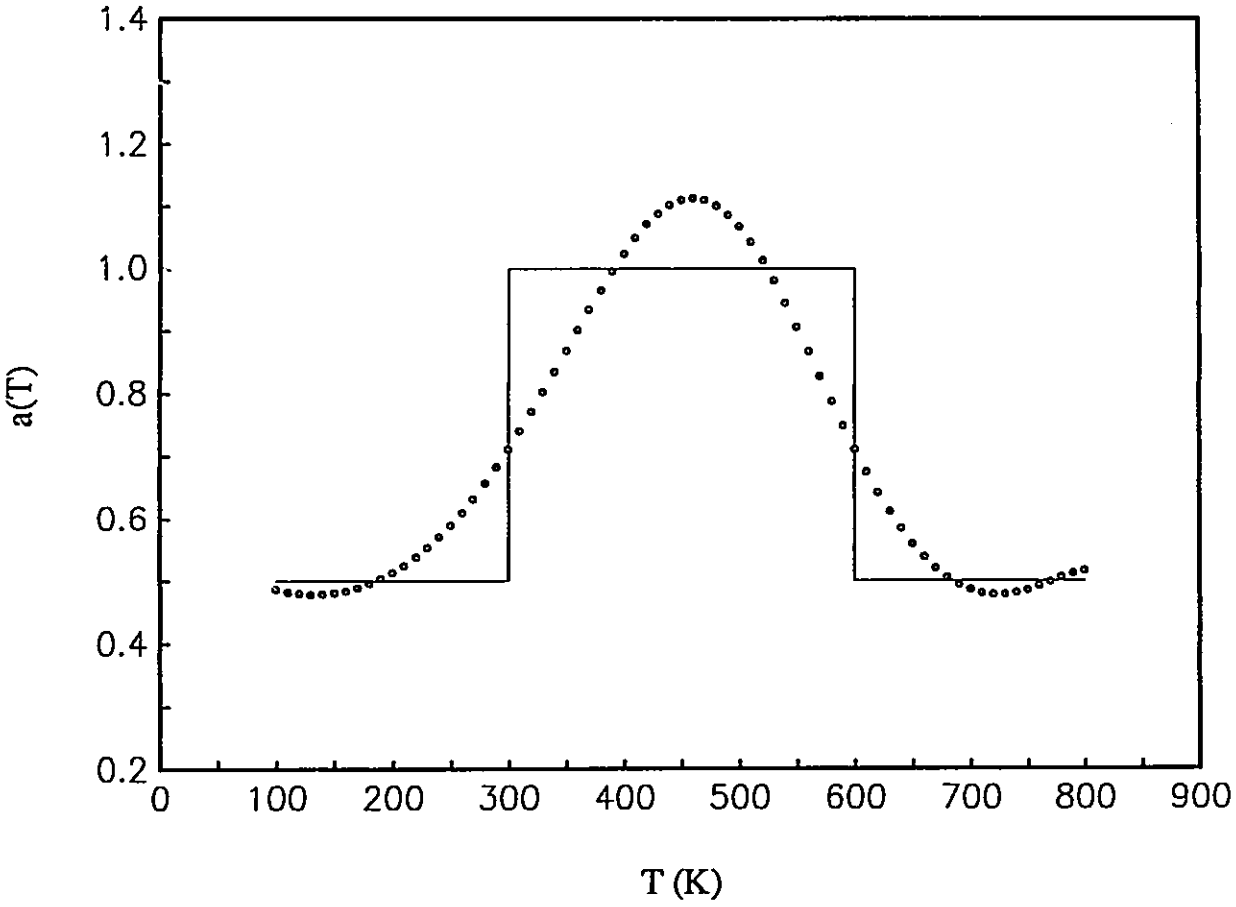

Fig. 4.3 Exact and computed temperature distributions for the rectangular distribution.

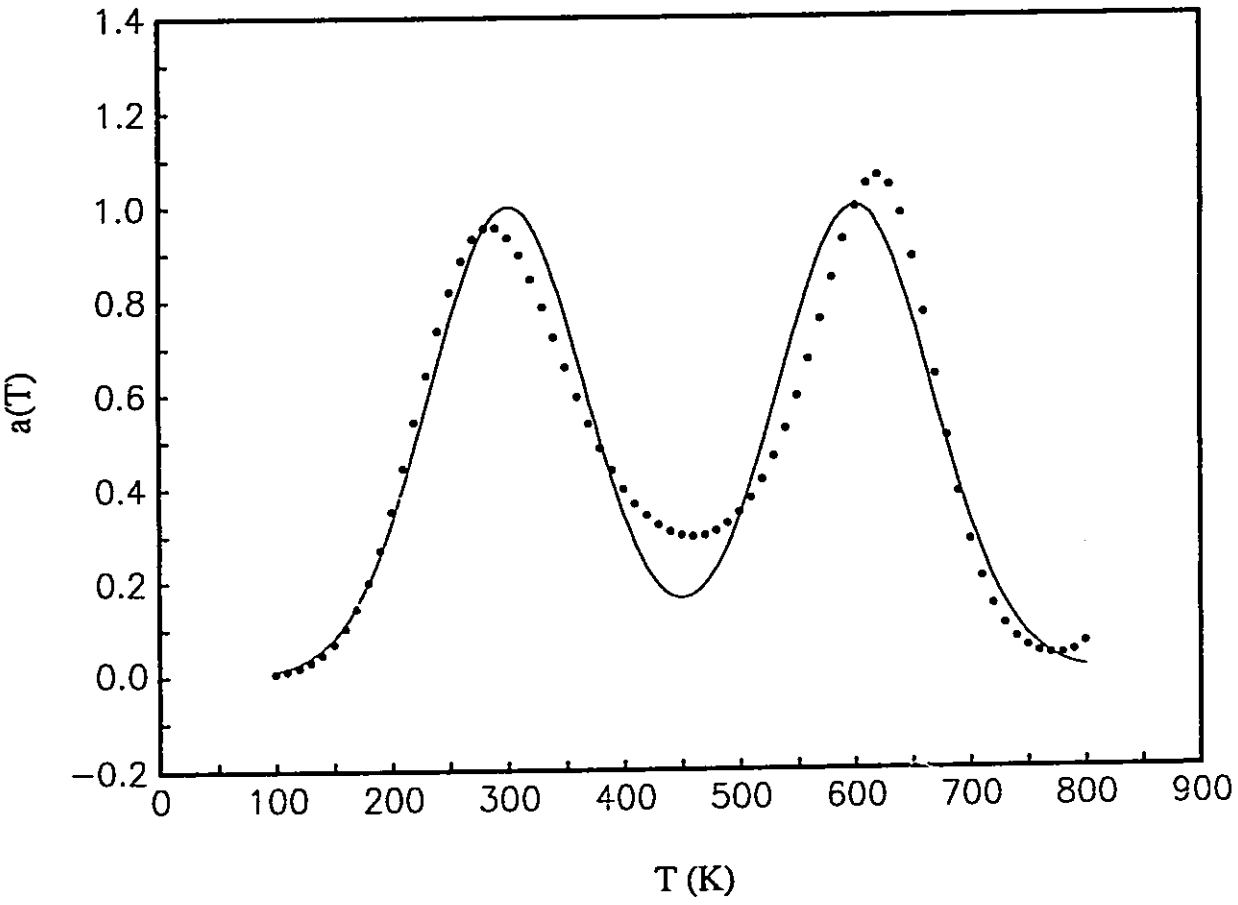

Fig. 4.4 Exact and computed temperature distributions for the double Gaussian distribution.

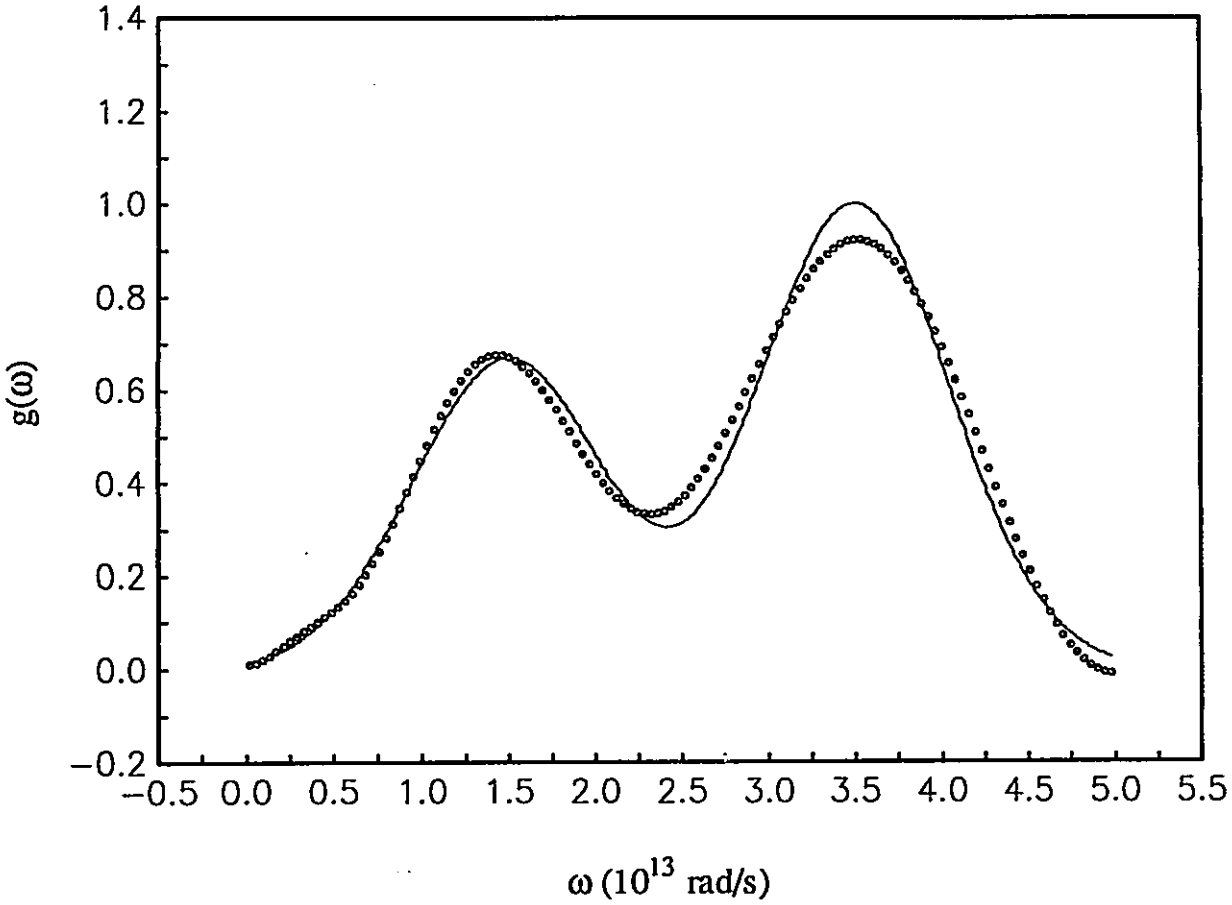

Fig. 4.5 Exact and computed phonon density of states distributions.

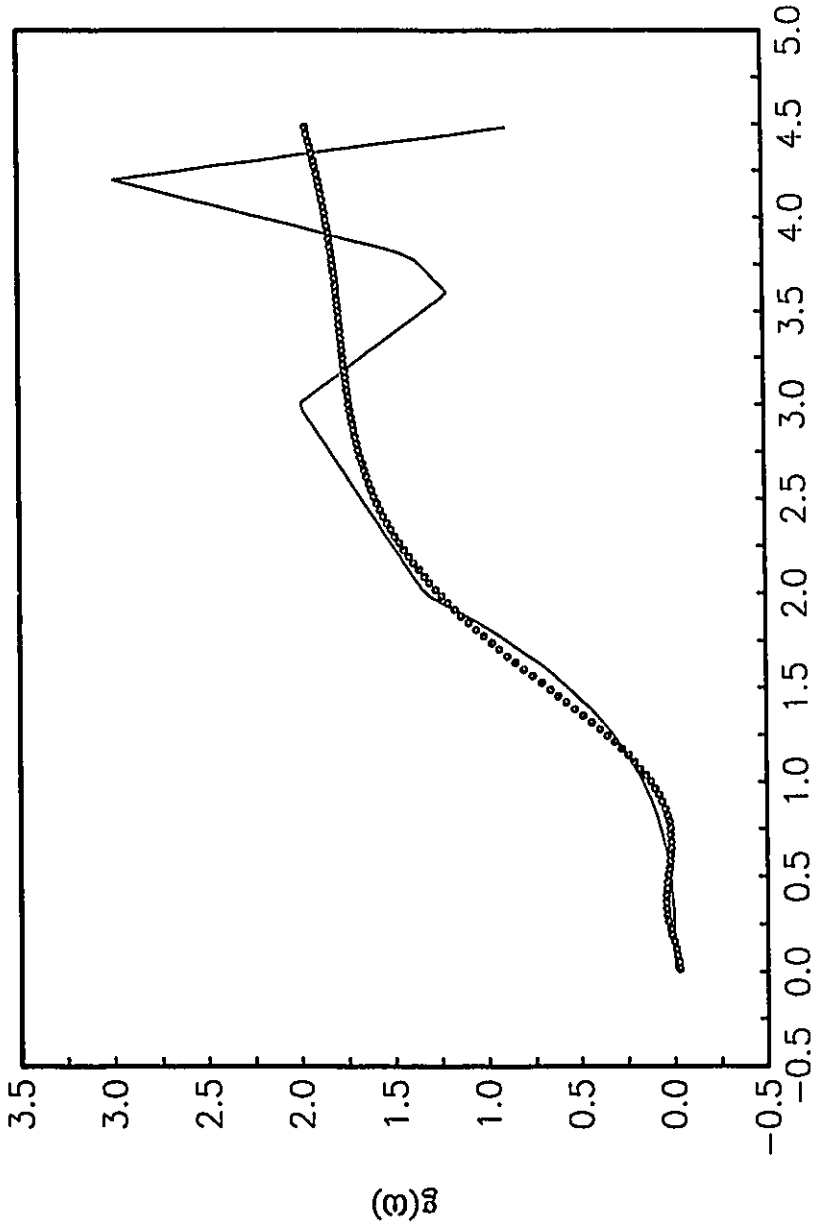

Fig. 4.6 Exact and computed phonon density of states distributions.

CHAPTER FIVE

Laplace Transform Method

1. Principle of the Laplace transform method

Consider Planck's law:

$$W(\nu) = \frac{2\,h\nu^3}{c^2} \int_0^{\infty} \frac{a(T)\,dT}{e^{h\nu/kT} - 1} \qquad (5.1)$$

Introducing the normalized absolute "coldness" u as

$$u = \left(\frac{h}{k}\right)\frac{1}{T} \quad \text{and} \quad a(u)du = -a(T)dT \qquad (5.2)$$

yields for (5.1)

$$W(\nu) = \frac{2\,h\nu^3}{c^2} \int_0^\infty \frac{\mathfrak{a}(u)\,du}{e^{u\nu} - 1} \tag{5.3}$$

where $\mathfrak{a}(u)$ is redefined as the area-coldness distribution of the black body. For convenience let $a(u) = \mathfrak{a}(u)$.

The kernel of the integral equation (5.3) can be rewritten as

$$\frac{1}{e^{u\nu} - 1} = \frac{e^{-u\nu}}{1 - e^{-u\nu}} = e^{-u\nu} \sum_{n=0}^{\infty} e^{-nu\nu} = \sum_{n=1}^{\infty} e^{-nu\nu}, \tag{5.4}$$

where the convergence of the series expansion in (5.4) is certain by virtue of $u\nu > 0$. Then Eq. (5.1) can be rewritten as

$$W(\nu) = \frac{2\,h\nu^3}{c^2} \int_0^\infty \sum_{n=1}^{\infty} e^{-nu\nu}\, a(u)\, du \tag{5.5}$$

Replacing the variable nu by u', i.e.,

$$u' = nu, \qquad du = \frac{1}{n}\, du' \tag{5.6}$$

thus

$$W(\nu) = \frac{2\, h\nu^3}{c^2} \int_0^{\infty} e^{-u'\nu} \sum_{n=1}^{\infty} \frac{1}{n}\, a\left(\frac{u'}{n}\right) du' \tag{5.7}$$

which, after replacing u' by u, yields

$$W(\nu) = \frac{2\, h\nu^3}{c^2} \int_0^{\infty} e^{-u\nu} \sum_{n=1}^{\infty} \frac{1}{n}\, a\left(\frac{u}{n}\right) du \tag{5.8}$$

$$\frac{c^2}{2\, h} \frac{W(\nu)}{\nu^3} = \int_0^{\infty} e^{-u\nu} \sum_{n=1}^{\infty} \frac{1}{n}\, a\left(\frac{u}{n}\right) du \tag{5.9}$$

Let

$$f(u) = \sum_{n=1}^{\infty} \frac{1}{n} a(\frac{u}{n}) \tag{5.10}$$

and

$$g(v) = \frac{c^2}{2h} \frac{W(v)}{v^3} \tag{5.11}$$

then

$$g(v) = \int_0^{\infty} e^{-uv} f(u)\, du \tag{5.12}$$

From (5.12), we see that f(u) is the inverse Laplace transform of g(v), i.e.

$$f(u) = L^{-1}[\, g(v)\,] \tag{5.13}$$

Bojarski[7] used an iterative procedure, choosing $L^{-1}[g(v)]$ as the first iterative value, thus

$$a_{m+1}(u) = f(u) - \sum_{n=2}^{m} \frac{1}{n} a(\frac{u}{n}) \tag{5.14}$$

$$a(u) = \lim_{m->\infty} a_m(u) \qquad (5.15)$$

Chen[10] also used the iterative procedure and presented an explicit series expression for the solution by using the modified Moebius formula. The final result is obtained as

$$a(u) = \sum_{n=1}^{\infty} \frac{\mu(n)}{n} f(\frac{u}{n}) \qquad (5.16)$$

where $\mu(n)$ are Moebius functions in the theory of numbers.

2. Application to the black body radiation problem

First consider the rectangular area-coldness distribution given by:

$$a(u) = H(u - u_1) - H(u - u_2) \qquad (5.17)$$

Here H is the Heaviside step function, $u_1 = 10$, $u_2 = 50$.

Then the power spectrum corresponding to the above distribution can be easily calculated as

$$W(\nu) = \frac{2h\nu^2}{c^2} [\ln(1 - e^{-u_2\nu}) - \ln(1 - e^{-u_1\nu})] \qquad (5.18)$$

Following the procedure described in the previous section, we have

$$f(u) = L^{-1}\{ \frac{1}{v} [\ln(1 - e^{-u_2 v}) - \ln(1 - e^{-u_1 v})]\} \qquad (5.19)$$

For this simple case the inverse Laplace transform will be done in two ways. One is analytic, another is numerical. Expanding the logarithmic terms and using the integration theorem of Laplace transforms, this becomes:

$$f_a(u) = \sum_{n=1}^{\infty} \frac{1}{n} [H(\frac{u}{n} - u_1) \cdots H(\frac{u}{n} - u_2)] \qquad (5.20)$$

This is shown in Fig. 5.1 with a dotted line. In the summation of (5.20) the maximum n is 200. This is a special case in that the f(u) can be found analytically. Generally, we must use a numerical method to do the inverse Laplace transform. Here Ang, Lund et al.'s[40], so called "Complex variable and regularization methods of inversion of the Laplace transform", inverse procedure is used. This method is based on a Sinc solution of the integral equation

$$\int_0^{\infty} f(t)e^{-st}dt = g(s)$$

via standard regularization. The numerical result is shown in Fig. 5.1 with a solid line. From Fig. 5.1, we can see the difference between $f_a(u)$ and $f_n(u)$.

Next the distribution a(u) is calculated using equation (5.16) based on the data $f_a(u)$ and $f_n(u)$ in Fig. 5.1 respectively. The comparison of $a_a(u)$ and $a_n(u)$ is shown in Fig. 5.2. By comparing $a_a(u)$ and $a_n(u)$, we can say that as long as f(u) is found precisely, the area-coldness distribution can be found precisely too by using the Moebius inverse formula. Obviously the main problem in the Laplace transform method is how to find a good numerical procedure to do the inverse Laplace transform. Actually this problem is another kind of Fredholm integral equation and is almost as difficult as the original one.

For comparison with regularization and maximum entropy methods, another numerical reconstruction is presented. The Gaussian area-coldness distribution is given by

$$a(u) = e^{-\frac{(u-50)^2}{80}} \qquad 0 \le u \le 100 \qquad (5.21)$$

The corresponding power spectrum is given by

$$W(\nu) = \frac{2h\nu^3}{c^2} \int_0^{100} \frac{e^{-\frac{(u-50)^2}{80}}}{e^{u\nu} - 1} du$$

Next the Laplace transform method described above is applied to obtain a(u) based on the 80 points of the discrete data W(v). In the summation of equation (5.16) the maximum n is 200. Fig. 5.3 shows the result. As we can see, comparing with the reconstructions by using either regularization method or maximum entropy method, these results are very poor.

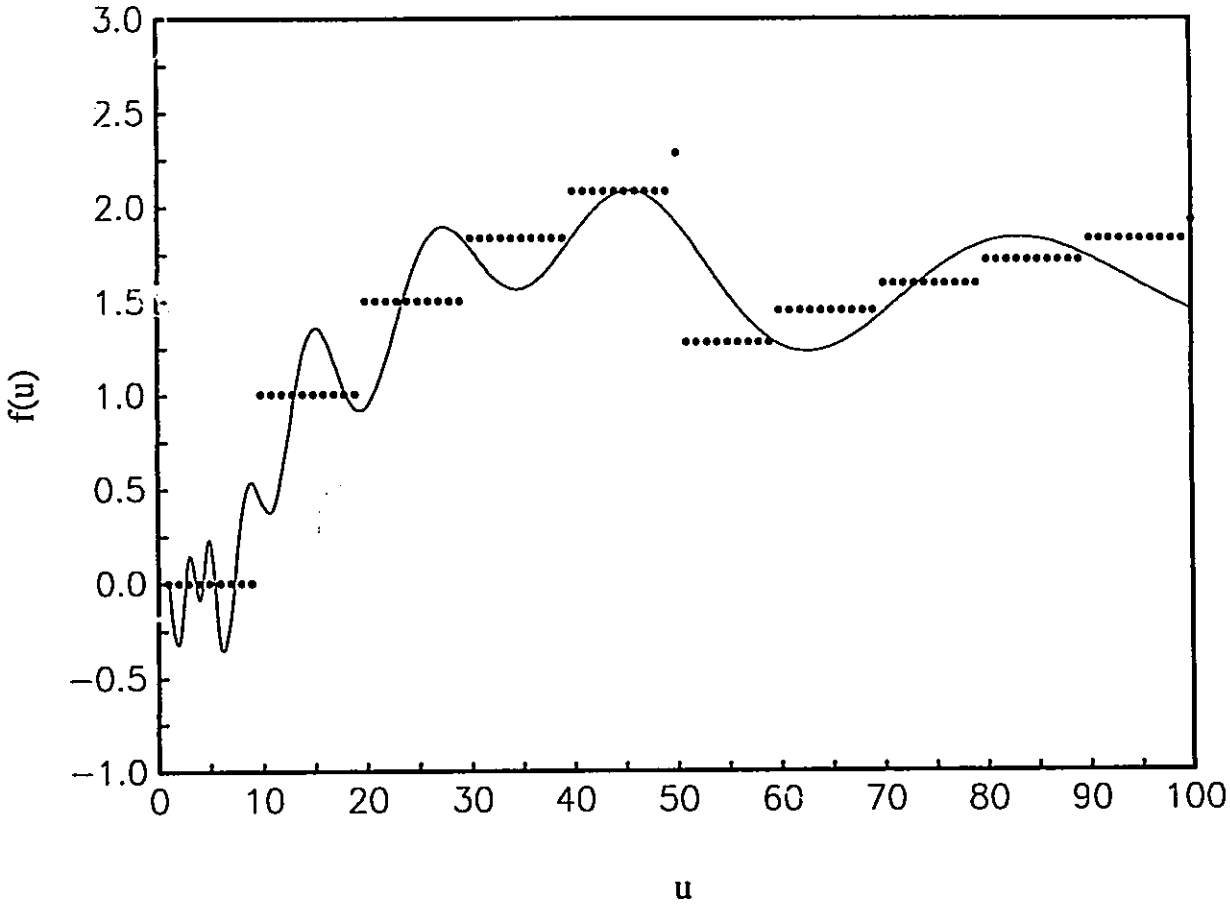

Fig. 5.1 Comparison between $f_a(u)$ (with dotted line) and $f_n(u)$ (with solid line).

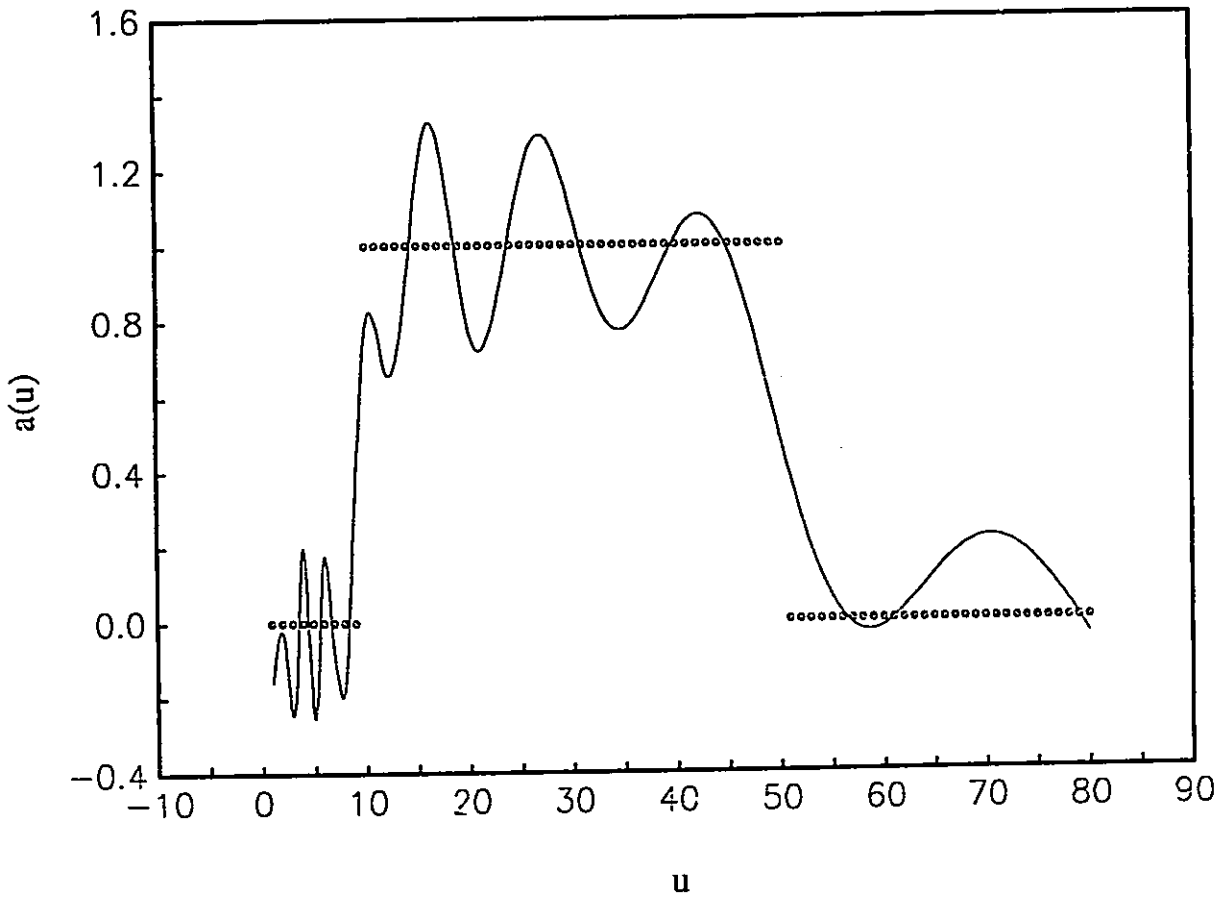

Fig. 5.2 Comparison between $a_a(u)$ (with dotted line) and $a_m(u)$ (with solid line).

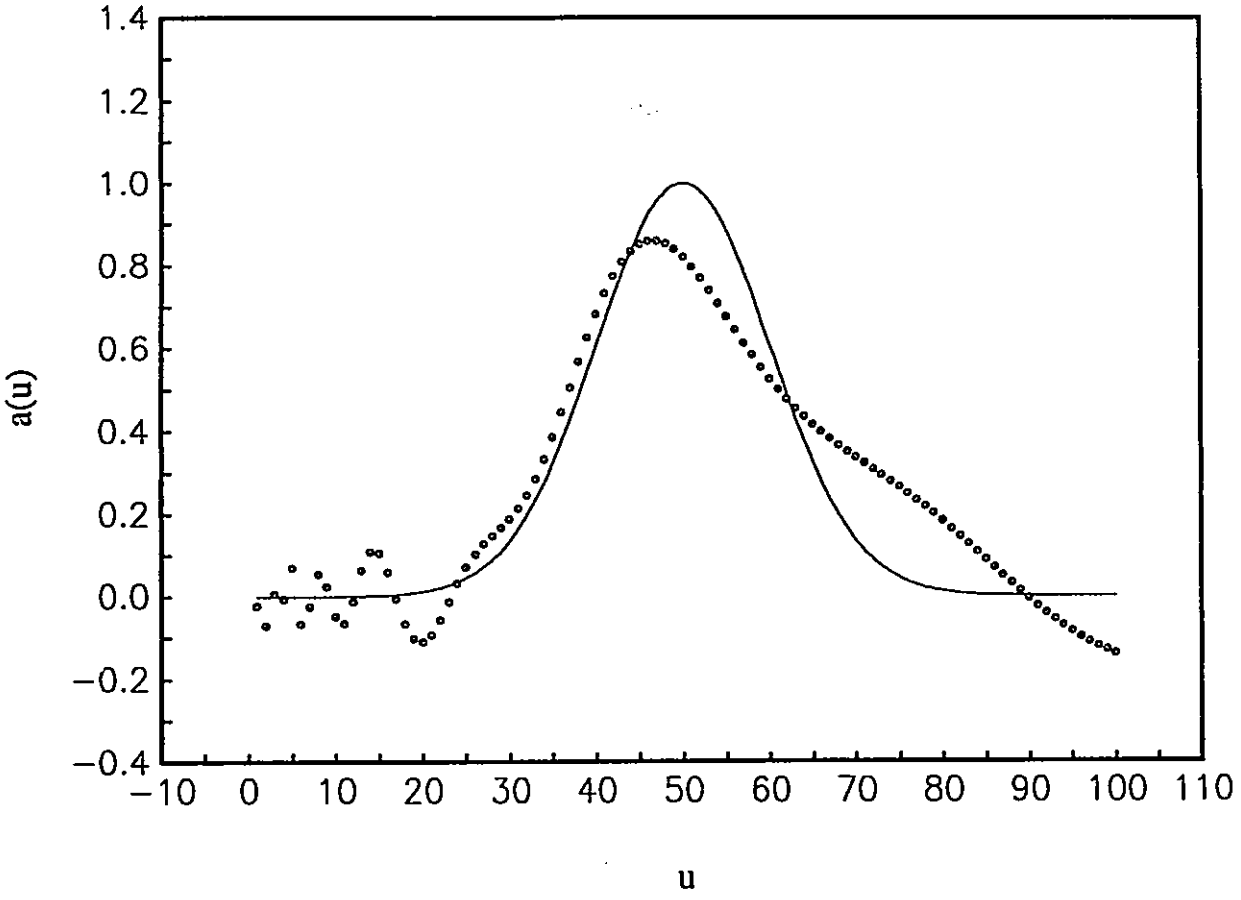

Fig. 5.3 Exact and computed coldness distributions for the Gaussion distibution.

CHAPTER SIX

Conclusion and Discussion

The inverse black body radiation problem and the phonon density of states problem we study here are ill-posed. The numerical solutions for the two problems are obtained successfully by implementing the regularization and the maximum entropy techniques. The regularization method is just the method which is designed to deal with these incorrectly posed problems. From the results presented in Chapter Three, it can be seen that this method is very efficient, especially for the reconstructions of smooth functions. Because the regularization procedure is based on the assumption that the sought function is a reasonably smooth function, it is not very efficient for the reconstructions of the sought functions which are not smooth or have some discontinuities. We can see this in Fig. 3.3, 3.4, 3.6, and 3.15. Here we also can see that the regularization parameter α and operator L do affect the results sensitively. How to choose α and L is still a problem. Generally when the noise in the input data increases, α should be increased. In this work α is chosen through doing numerical experiments. There is a method called GCV(Generalized Cross-Validation)[41] which can be used to

compute this parameter. So far we haven't tried it. There is no way to tell its advantages and disadvantages. As for the regularization parameter L, for the smooth sought functions, a higher order regularization parameter should be chosen. This means that we need some pre-information about the sought functions. Sometimes this is a big restriction to real systems. So it is still necessary to investigate how the regularization parameter α and the regularization operator L affect the results theoretically.

The maximum entropy method for solving both the inverse black body radiation problem and phonon density of states problem is totally different from previous methods, and offers a number of advantages. The problems of existence and uniqueness have already been solved. The procedure is relatively straight-forward in that one must simply search for the minimum of the potential function defined in Eq. (4.16). There are no associated regularization parameters, and no uncertainties in the computed deconvolution, as in other procedures. The main difficulty with the entropy technique is in the determination of the global minimum of the potential function Γ. We must determine the set of parameters λ_i, which produce this minimum. One also has the freedom of choosing different numbers of parameters, and different initial values in the search for this minimum. Obviously the larger the number of parameters, the better the fit that one can achieve. However the process of determining that fit becomes increasingly difficult. While the results which we obtain using the maximum entropy method for some reconstructions are not as good as those obtained using regularization or deconvolution, we have no parameters or uncertainties to affect the results. If the global minimum can be found, the only variables in this approach are the number of parameters and the functions $M_n(x)$. Comparing the regularization method and the maximum entropy method with the Laplace transform method, we can see that the Laplace transform method is much poorer than the regularization and maximum entropy methods.

Actually solving for the inverse Laplace transform is as difficult as solving the original problem, because inverting a Laplace transform is an ill-posed problem too. Both the regularization method and the maximum entropy method are suitable not only for the inverse black body radiation and phonon density of states problems, but also for a large number of Fredholm integral equations of the first kind in physics.

References:

[1] A. N. Tikhonov, Soviet Math. Dolk., **4**, 1035(1963).

[2] A, N. Tikhonov, Soviet Math. Dolk., **4**, 1634(1963).

[3] D. L. Phillips, J. ACM, **9**, 84(1962).

[4] X. G. Sun and K. L. Jaggard, J. Appl. Phys., **62**, 4382(1987).

[5] C. Shannon, Bell. Syst. Tech J., **27**, 379 and 623(1948).

[6] A. N. Tikhonov and V. Y. Arsenin, *Solution of ill-posed problems*.(Winston-Wiley, New York, 1977).

[7] N. N. Bojarski, IEEE Trans. Antennas Propag., **AP-30**, 778(1982).

[8] M. Hamid and H. A. Ragheb, IEEE Trans. Anennas Propag., **AP-31**, 810(1983).

[9] N. N. Bojarski, IEEE Trans. Antennas Propag., **AP-32**, 415(1984).

[10] M. N. Lakhtakia and A. Lakhtakia, IEEE Trans. Antennas Propag., **AP-32**, 872(1984).

[11] N. N. Bojarski, M. N. Lakhtakia and A. Lakhtakia, IEEE Trans. Antennas Propag., **AP-33**, 226(1985).

[12] J. D. Hunter, IEEE Trans. Antennas Propag., **AP-34**, 261(1986).

[13] H. A. Ragheb and M. Hamid, IEEE Trans. Antennas Propag., **AP-35**, 739(1987).

[14] Y. Kim and D. L. Jaggard, IEEE Trans. Antennas Propag., **AP-33**, 797(1985).

[15] N. X. Chen, Phys. Rev. Lett., **64**, 1193(1990).

[16] N. X. Chen and G. Y. Li, IEEE Trans. Antennas Propag., **38**, 1287(1990).

[17] E. W. Montroll, J. Chem. Phys., **10**, 218(1942).

[18] H. Grayson-Smith and J. P. Stanley, J. Chem. Phys., **18**, 236(1950).

[19] W. Kroll, Progr. Theor. Phys. Japan, **8**, 457(1952).

[20] G. Weiss, Progr. Theor. Phys Japan, **22**, 526(1959).

[21] R. G. Chambers, Proc. Phys. Soc. **78**, 941(1961).

[22] A. Junod, T. Jarlborg and J. Muller, Phys, Rev. B, **27**, 1568(1983).

[23] J. W. Loram, J. Phys, C: Solid State Phys., **19**, 6113(1986).

[24] W. C. Kok, Solid State Comm., **74**, 843(1990).

[25] N. X, Chen, Y. Chen and G. Li, Phys. Lett. A, **149**, 357(1990).

[26] A. J. Pindor, In Morden Trends in the Theory of Condensed Matter, **115**, 563(Springer-Verlag, Berlin, 1980).

[27] J. Igalson, A. J. Pindor and L. Sniadower, J. Phys. F, **11**, 995(1981).

[28] The IMSL libraries *Problem-solving software system for numerical FORTRAN programming*

[29] E. T. Jaynes, Phys. Rev., **106**, 620(1957).

[30] E. T. Jaynes, Phys. Rev., **108**, 171(1957).

[31] C. R. Smith, R. Inguva and R. L. Margan, Maximum entropy inverse in physics, SIMA-AMS Proceedings, **14**, 127(1984).

[32] R. Inguva and J.Baker-Jarvis, "Maximum entropy and inverse scattering", *in maximum entropy and Bayesian method in applied statistics*, p.300(Cambridge, London, 1986)

[33] J. Baker-Jarvis, J. Math. Phys. **30**, 302(1989).

[34] J. Baker-Jarvis, J. Alameddine and D. Schultz, Numerical methods for partial differential equations, **5**, 133(Wiley, New York, 1989).

[35] J. Baker-Jarvis, M. Racine and J. Alameddine, J. Math. Phys. **30**, 1459(1989).

[36] L. R. Mead and N. Papanicolaou, J. Math. Phys., **25**, 2404(1984).

[37] L. R. Mead, J. Math. Phys., **27**, 2903(1986).

[38] J. E. Gubernatis, M. Jarrell, R. N. Silver and D. S. Sivia, Phys. Rev. B., **44**, 6011(1991).

[39] MINUIT *Function minimization and error analysis* Release 89.12j. F. James, M. Roos.

[40] D. D. Ang, J. Lund and F. Stenger, Mathematics of Computation, **53**, 589(1989).

[41] G. H. Golub and M. Heath, Technometrics, **21**, 215(1979).